INFORMATION TO USERS

This manuscript has been reproduced from the microfilm master. UMI films the text directly from the original or copy submitted. Thus, some thesis and dissertation copies are in typewriter face, while others may be from any type of computer printer.

The quality of this reproduction is dependent upon the quality of the copy submitted. Broken or indistinct print, colored or poor quality illustrations and photographs, print bleedthrough, substandard margins, and improper alignment can adversely affect reproduction.

In the unlikely event that the author did not send UMI a complete manuscript and there are missing pages, these will be noted. Also, if unauthorized copyright material had to be removed, a note will indicate the deletion.

Oversize materials (e.g., maps, drawings, charts) are reproduced by sectioning the original, beginning at the upper left-hand corner and continuing from left to right in equal sections with small overlaps.

Photographs included in the original manuscript have been reproduced xerographically in this copy. Higher quality 6" x 9" black and white photographic prints are available for any photographs or illustrations appearing in this copy for an additional charge. Contact UMI directly to order.

Bell & Howell Information and Learning
300 North Zeeb Road, Ann Arbor, MI 48106-1346 USA
800-521-0600

Connexins 26 and 32 in the Developing Neocortex

James L. Eubanks

A dissertation submitted in partial fulfillment of the requirements for the degree of

Doctor of Philosophy

University of Washington

2000

Program Authorized to Offer Degree: Neurobiology and Behavior

Bell & Howell Information and Learning Company
300 North Zeeb Road
P.O. Box 1346
Ann Arbor, MI 48106-1346

In presenting this dissertation in partial fulfillment of the requirements for the Doctoral degree at the University of Washington, I agree that the Library shall make its copies freely available for inspection. I further agree that extensive copying of the dissertation is allowable only for scholarly purposes, consistent with "fair use" as prescribed in the U.S. Copyright Law. Requests for copying or reproduction of this dissertation may be referred to Bell and Howell Information and Learning, 300 North Zeeb Road, Ann Arbor, MI 48106-1346, to whom the author has granted "the right to reproduce and sell (a) copies of the manuscript in microform and/or (b) printed copies of the manuscript made from microform."

Signature: 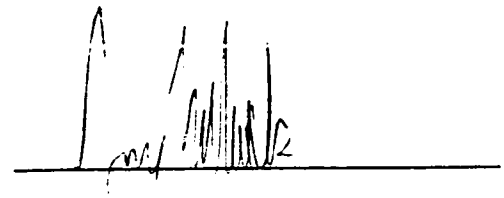

Date: 11/1/00

University of Washington
Graduate School

This is to certify that I have examined this copy of a doctoral dissertation by

James L. Eubanks

and have found that it is complete and satisfactory in all respects.
and that any and all revisions required by the final
examining committee have been made.

Chair of Supervisory Committee:

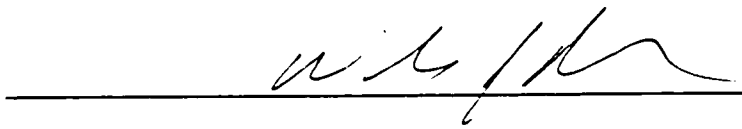

William J. Moody

Reading Committee:

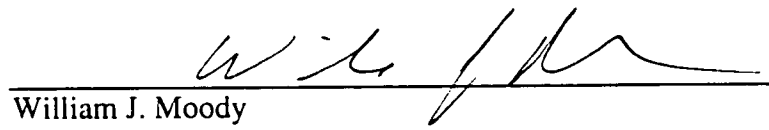

William J. Moody

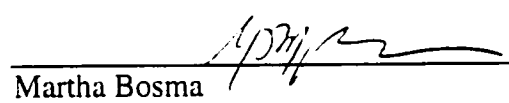

Martha Bosma

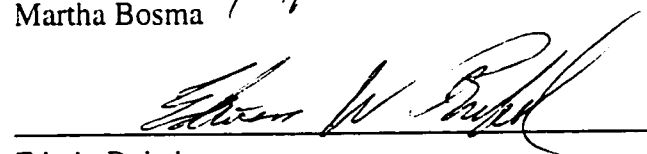

Edwin Rubel

Date: Nov 1, 2000

University of Washington

Abstract

Connexins 26 and 32 in the Developing Neocortex

James L. Eubanks

Chairperson of the Supervisory Committee:

Professor William J. Moody
Zoology

During neocortical neurogenesis, the basic structure of the neocortex arises through a precise coordination of cell division, specification, migration, and circuit formation. These processes are influenced, if not defined, by cell-cell interactions. Gap junctions—transmembrane proteins that allow direct electrical or biochemical communication between cells— are a prevalent and important mode of cell-cell signaling throughout neocortical development. Gap junction channels are composed of 12 connexin subunits and may display different signaling properties depending on which connexins are present. We investigated the expression of two connexin subunits, Cx26 and Cx32, during neocortical neurogenesis in the mouse, a period spanning embryonic days 12 and 17 (E12-E17). The purpose of our initial study was to elucidate possible developmental roles for Cx26 and Cx32 by comparing their expression patterns in populations of cells undergoing distinct developmental events: proliferation, migration, or differentiation. We found that Cx26 and Cx32 are both expressed throughout neocortical neurogenesis in all three populations of cells. This spatial and temporal overlap in expression suggests the possible formation of Cx26/Cx32 heteromeric channels, a well described channel configuration with distinct properties. However, through most of neurogenesis, Cx26 shows significant variation in expression between proliferating, migrating, and differentiating cells while Cx32 expression remains relatively uniform. In our second study, we addressed more directly the possible developmental role for Cx32 by examining the neocortex of Cx32 null embryos at E17,

the culmination of neurogenesis. We analyzed the embryos using a series of established histological and immunological markers of neocortical development and found no apparent disruption of normal neocortical development in the absence of Cx32. We did, however, find evidence for an up-regulation of Cx26 expression in Cx32 null neocortex. This result, in addition to suggesting a possible mechanism for compensation, attests to the importance of gap junctional communication to normal neocortical development In a third study, we discovered and isolated DECORE. a cortex specific protein that may be involved in the development of distinct neocortical layers.

TABLE OF CONTENTS

LIST OF FIGURES

LIST OF TABLES

Number Page

Introduction

The human cerebral cortex —with several billion neurons, each making more than a thousand synaptic connections— is regarded as one of the most complex objects in existence. Yet despite this daunting complexity, the developmental events involved in building the cerebral cortex are relatively well understood. In the mouse the predominant model for studying mammalian brain development—neurons of the neocortex[1] are produced through approximately 11 cycles of cell division in the final third of gestation (Caviness, Takahashi et al. 1995). During this developmental period, referred to as neocortical neurogenesis, newly formed neurons also undergo a well-defined pattern of migration and differentiation that will form six distinct layers in the adult neocortex.

An important feature of the developing neocortex is that discrete developmental processes (cell division, migration, and differentiation) take place in distinct, anatomically defined regions. Neuronal precursors in the ventricular zone (VZ), the proliferative region of the neocortex, show characteristic movements in which a cell's position varies with respect to its phase in the cell cycle. Upon exiting the cell cycle, neuronal precursors leave the VZ, migrate through the intermediate zone (IZ), and occupy the cortical plate (CP). Each subsequent wave of neurons migrates past the last, resulting in an inside-out pattern of development. With this pattern, the birth date of a neuron determines the cortical layer (II-VI) in which it ultimately resides (McConnell 1995; McConnell 1995).

Less well understood are the controls underlying neocortical neurogenesis that allow it to occur with a high level of fidelity. Studies involving heterotypic and heterochronic transplants have shown that the fate of a cell in the neocortex is influenced, to varying degrees, by its environment (See McConnell 1995 for review). As such,

[1] The term neocortex will be used through the remainder of this dissertation. The neocortex is the predominant structure of the forebrain that is often referred to as cerebral cortex. The cerebral cortex is actually comprised of neocortex, archicortex (olfactory cortex) and paleocortex (hippocampus). The neocortex has a six-layered structure that is unique to mammals. Hence the "neo" prefix denotes a more recent evolutionary origin.

developmental processes are largely shaped by cell-cell interactions. Intercellular signaling is known to take many forms in neocortical development including selective adhesion (Rakic and Caviness 1995) (Stoykova, Gotz et al. 1997), release of growth factors and cytokines (Ghosh and Greenberg 1995) and neurotransmitter signaling (LoTurco and Kriegstein 1995; Barker, Behar et al. 1998; Behar, Schaffner et al. 1998; Behar, Scott et al. 1999). Another important mode of cell-cell interaction was discovered through the observation that certain populations of cells in the developing neocortex are dye-coupled (Lo Turco and Kriegstein 1991; Peinado, Yuste et al. 1993). When one cell was injected with a tracer such as Neurobiotin or Lucifer yellow, the tracer spread to 50 or more cells, revealing an organization of coupled clusters. The cellular structures underlying dye coupling are gap junctions, trans-membrane proteins that form channels at points of contact between cells. Gap junctions allow the passage of ions and small molecules up to approximately 1 kDa (Bruzzone, White et al. 1996) (Bruzzone and Ressot 1997), thereby providing a direct route for cell-cell communication through electrical signaling or through the sharing of metabolites and signaling molecules. The formation of gap junction coupled cell clusters in the developing neocortex may therefore represent a means of coordinating and perhaps synchronizing the developmental processes of the cells contained within them.

The key to understanding the signaling properties of gap junctions likely rests in the details of their molecular structure. A functional gap junction is composed of 12 connexin subunits, with 6 connexins forming a hemi-channel, or connexon, in each adjacent cell. In rodents, 17 different connexins have been identified, each encoded by a separate gene (Dermietzel and et al. 1998). *In vitro* expression studies have demonstrated that several of these different connexins are able to co-assemble into functional heteromeric channels that show unique selectivity and gating properties, distinct from those of the corresponding homomeric channels composed of only one connexin type (Bruzzone and Ressot 1997) (Bevans, Kordel et al. 1998). Many cell types co-express multiple connexins (Risek, Klier et al. 1994) and immunoprecipitation studies have confirmed that different connexins co-assemble into both homomeric and heteromeric

channels *in vivo*. The emerging picture is one in which the pattern of connexin expression is a major factor in mediating the nature and extent of gap junctional coupling.

The most abundant and well-studied connexins in the neocortex are connexins 26,32,and 43 (Cx26, Cx32, and Cx43), all named for their molecular weights in kilodaltons. Previous studies have described the expression patterns of Cx26, Cx32, and Cx43 in the developing rat neocortex (Dermietzel, Traub et al. 1989; Dermietzel et al. 1993; Nadarajah, Jones et al. 1997). Cx26 and Cx43 were found to be the predominant isoforms expressed during the period of neurogenesis. After neurogenesis, in postnatal stages P7 to P28, the authors observed that Cx26 expression diminished and was largely replaced by abundant Cx32 expression throughout the neocortex. Cx43 expression levels remained relatively constant through both neurogenesis and post-natal development.

We undertook an analysis of connexin expression in the mouse neocortex during neurogenesis to complement our parallel studies of cell electrical properties and to lay the foundation for subsequent genetic analyses. Our initial results showed robust expression of Cx26 and Cx32, a surprising result given that Cx32 was not observed in previous analyses during neocortical neurogenesis in the rat. We chose to focus our subsequent analyses on the expression of Cx26 and Cx32 for two reasons. First, our observation of Cx32 expression during neurogenesis represented a novel finding worthy of further investigation. Second, Cx26 and Cx32, when co-assembled into heteromeric channels, show unique but well understood properties that may help shed light on cell-cell interactions underlying neurogenesis. Among these unique properties are electrical rectification and specificity with respect to the passage of second messengers (Barrio, Suchyna et al. 1991; Bukauskas, Elfgang et al. 1995).

In our first study reported in Chapter 2, we sought to ascertain the expression patterns of Cx26 and Cx32 within the context of the well-described developmental events during neocortical neurogenesis. In addition to labeling Cx26 and Cx32, we used established markers at each stage to identify the associated developmental events: Tuj1 as a marker of neuronal differentiation and BrdU incorporation studies to label cells in S-phase. As mentioned above, a fortuitous feature of the developing neocortex is that the

VZ, IZ, and CP represent discrete, morphologically distinct regions. Thus, with our markers, a coronal cross section of the embryonic neocortex allowed us to observe Cx26 and Cx32 expression in conjunction with the definitive events of neurogenesis: cell proliferation, neuronal migration, and neuronal differentiation.

We find that Cx26 and Cx32 are both expressed in the VZ, IZ, and CP of the mouse neocortex throughout neurogenesis, but their patterns diverge markedly around E17. Quantitative analyses of connexin immunostaining indicate that 1. Cx26 and Cx32 each show significant differences in expression among dividing, migrating, or differentiating cell populations, to varying degrees by stage and 2. At certain stages, Cx26 and Cx32 show overlapping expression patterns consistent with the possible formation of heteromeric channels.

In Chapter 3, we describe our investigation into possible roles for Cx32 in neocortical development by examining brains of Cx32 null mice at E17, the culmination of neocortical neurogenesis. Using a battery of established immunological and histological markers, we compared developmental parameters in Cx32 null neocortex with those of their wild type and heterozygote littermates. We found no gross differences in indicators of cell proliferation, migration, or differentiation between the three genotypes. We did, however, find preliminary evidence for a compensatory increase in Cx26 expression in Cx32 null neocortex.

Chapter 4 chronicles our discovery of DECORE, a novel developmentally expressed protein specific to cortex. We report the developmental expression pattern of DECORE and our isolation and initial characterization of the protein.

Chapter 1

Materials and Methods

A. General Methods:

Tissue Preparation: Timed pregnant C57/Bl6 mice were acquired from a commercial supplier. Mice were mated overnight by the commercial facility and pregnancy was confirmed in the morning by the presence of a vaginal plug. The first day of confirmed pregnancy was designated embryonic day zero (E0). All procedures involving mice were conducted according to the guidelines of the University of Washington Animal Care Committee, with an emphasis on minimizing pain and discomfort to the animals. Mice were euthanized in a CO_2 chamber at the gestational ages specified. Uteri were removed trans-abdominally and immediately placed in ice cold artificial cerebrospinal fluid (ACSF; 119 mM NaCl, 2.5 mM KCl, 1.3 mM $MgCl_2$, 2.5 mM $CaCl_2$, 1.0 mM NaH_2PO_4, 26.2 mM $NaHCO_3$, 11mM D-glucose) bubbled with 95% O_2/5%CO_2. Pups were removed and forebrains were fixed in either 2% Paraformaldehyde (PFA) in phosphate buffered saline (PBS) or PLP fix (2% PFA in PBS containing 75mM L-lysine and 100mM sodium periodate) for 30-60 minutes at room temperature. After fixation, tissue was placed in 12.5% sucrose in PBS overnight at 4 degrees C. Tissue was frozen in liquid nitrogen and 12uM sections were cut on a cryostat. Consecutive sections were mounted on a series of slides so that immunostaining from multiple antigens could be examined in adjacent sections from the same brain

Western blotting: Tissue was prepared as described previously (Nadarajah, Jones et al. 1997) for detection of Cx26 and Cx32 in immunoblots. Briefly, forebrains were removed from 6 E17 embryos as described above and 1g of liver tissue was removed from an adult mouse (the mother of the embryos) as a positive control. Tissues were intermittently homogenized and sonicated in 20mM $NaHCO_3$ containing 1uM PMSF and 10ug/ml each of leupeptin, pepstatin A, and aprotinin. Membrane fractions were enriched by extraction with 20mM NaOH and subsequent centrifugation. Protein concentrations were estimated

by UV spectrophotometry. Approximately 100ug of protein per lane was run on a 4-16% SDS PAGE gradient gel with molecular weight markers in alternate lanes (14-150 kD color markers, Sigma). Gels were subsequently transferred to nitrocellulose membranes using the semi-dry method (Biorad). Blots were pre-blocked by incubating in TBSTM (0.1M tris-buffered saline with 2% w/v dried milk (Carnation) and 0.05% v/v Triton-X (Sigma)) for 1 hour at room temperature. The blots were then incubated overnight in polyclonal rabbit anti-Cx26 or anti-Cx32 (both from Zymed, #51-2800 and #71-0600, respectively) diluted 1:500 (1.0 ug/ml) in TBSTM. For the Cx32 blocking peptide control, the anti-Cx32 antibody (1.0 ug/ml) was pre-incubated with the Cx32 blocking peptide (5.0 ug/ml provided by the manufacturer (Zymed). After a series of rinses in TBSTM, blots were incubated for 45 minutes in alkaline phosphatase conjugated goat anti-rabbit diluted 1:7500 (Promega, Inc.). The blots were then rinsed with TBS and developed in alkaline phosphatase buffer with NBT/BCIP (0.1M tris, pH 9.5, 0.1mM NaCl, 5mM $MgCl_2$, 1mg/ml NBT, and 0.25 mg/ml BCIP). (Nadarajah, Jones et al. 1997; Mambetisaeva, Gire et al. 1999).

Immunocytochemistry: Sections were processed for immunocytochemistry as follows. All incubations were at room temperature: 20 minutes in dilution/blocking buffer (DBB; 3% normal goat serum, 2% bovine serum albumen, and 0.2% Triton-X in 0.1M tris-buffered saline (TBS)), overnight in primary antibody (rabbit anti-Cx26 10ug/ml or rabbit anti-Cx32 5ug/ml, Zymed, Inc.), 1 hour in biotinylated secondary antibody (goat anti-rabbit 3.75 ug/ml in DBB, Vector, Inc.), and 1 hour in FITC conjugated avidin (20mg/ml in TBS pH 8.0 Vector, Inc.) Cx32 blocking peptide controls were run as above, except the anti-Cx32 antibody (5ug/ml) was preincubated with Cx32 blocking peptide at a concentration of 20ug/ml. All immunostained sections were run in parallel with a negative control in which the primary antibody was omitted. In no circumstances did background staining resemble or interfere with specific labeling.

B. Specific Methods by Chapter:

Chapter 2:

BrdU labeling:To label proliferative cells in S-phase, timed pregnant mice were injected 30-45 minutes before sacrifice with 50ug BrdU in sterile saline per gram of body weight. Tissue was dissected, fixed and sectioned as outlined above. For double labeling for neuron-specific tubulin (TUJ1) and BrdU, sections were first incubated in affinity purified polyclonal TUJ1 (1 ug/ml in DBB, BabCo, Inc.) overnight followed by a 1hour incubation with Texas Red conjugated goat anti-rabbit antibody (5ug/ml). The samples were then treated with 2N HCl for 1 hour, followed by a 1 hour incubation in mouse anti-BrdU supernatant (G3G4) at approximately 25ug IgG/ml in DBB (antibody G3G4 was developed by Dr. S.J. Kaufman and obtained from the Developmental Studies Hybridoma Bank) and 1hour in FITC conjugated goat anti-mouse (28 mg/ml) in DBB (Jackson, Inc.).

Image capture and analysis: Digital images were acquired using a 3-chip color camera (Optronics, Inc.) through a microscope (AxioSkop Zeiss, Inc) with a 63X oil immersion objective (Fluoroplan, Zeiss, Inc.) and the appropriate fluorescent filters (Chroma, Inc.). Composite Images were assembled using Canvas (Deneba, Inc.) and Adobe Photoshop software (Adobe, Inc.). Analyses of Cx26 and Cx32 immunoreactivity patterns were performed on adjacent sections at E12 (n=5 brains from 3 litters), E14 (n=6 brains from 3 litters), and E16 (n=5 brains from 2 litters). For this analysis, images of adjacent Cx26 and Cx32 fluorescent immunostained sections of the cerebral wall were converted to a 0 to 255 grayscale and inverted using Scion Image software (Scion, Inc.). Using the same software, the sections were measured and divided into 10 bins whose height was 10% of the ventricular to pial distance and whose width was 100uM. The average gray value was then measured for each bin. The data were exported to a spreadsheet for subsequent statistical analyses.

Chapter 3:

Cx32 null mice: Embryonic day 17 Cx32 null mice were a generous gift of Klaus Willecke. The Cx32 null mouse line was constructed as described previously (PNAS paper). The embryos were dissected and brains processed using the protocol from Chapter 2. The brains were kept in 12% sucrose in PBS and shipped overnight on ice from Bonn,Germany. PCR genotyping was performed by Thomas Ott at Universitat Bonn, using tail clips from the mouse embryos and the published PCR protocol (cite). The litter used in our analyses contained two homozygous null mice, two wild-types, and three heterozygotes. At the University of Washington, the tissue was frozen with liquid nitrogen, 12 uM coronal cryostat sections were taken, and immunohistochemical analyses were performed..In sectioning, special attention was paid to rostrocaudal position of coronal sections in order to allow accurate anatomical comparisons between brains. Accordingly, slides from each brain were numbered to reflect their relative positions in the rostrocaudal plane.

Immunohistochemistry for analysis of Cx32 null mice: Immunofluorescent staining was performed using the basic protocol outlined in Chapter 2. Listed below are the primary antibodies used and their working concentrations: Rabbit anti-Calretinin (Chemicon. #) *ug/ml, Rabbit anti-Cx26 (Zymed 51----) 5 ug/ml, Rabbit anti-Cx43 (Zymed **) 5 ug/ml, Mouse RC2 IgM (Radial glial cell marker; Developmental Studies Hybridoma Bank) supernatant diluted 1:1 (approximately 25 ug/ml), Rabbit anti-Phosphohistone-3 (Company?) conc used?, Mouse anti-Tuj1 (Neuron-specific tubulin; Babco #***) conc used? Rabbit anti-Type II voltage gated sodium channel Alpha subunit (Chemicon #) 5ug/ml. An overnight incubation with specific primary antibodies was followed by a 1 hour incubation with the appropriate secondary antibody. For primary antibodies raised in rabbit, we used a biotinylated goat anti-rabbit (Vector #) at conc? followed by avidin conjugated FITC (conc). Following mouse primary antibodies, we used FITC or Texas Red goat anti-mouse at conc. All immunostained sections were counterstained with

DAPI (1uM) during the final rinses. Slides were coverslipped using Vectashield (Vector) before digital micrographs were obtained.

Chapter 4:

Triple label immunocytochemistry: Sections of brains fixed with PLP were processed for double labeling for Cx32 and RC-2, a marker for radial glia (RC-2 was developed by Dr. M. Yamamoto and obtained from the Developmental Studies Hybridoma Bank, maintained by the University of Iowa). These samples were processed as above, but with the simultaneous incubation with the anti-Cx32 antibody from the lot which recognizes DECORE (Zymed lot #***5 ug/ml) and mouse anti-RC-2 supernatant (approx. 25 ug IgG/ml). Likewise, sections were co-incubated for 1hour with the appropriate secondary antibodies (biotinylated goat anti-rabbit + Texas Red conjugated goat anti-mouse 10 ug/ml, Jackson,Inc.) For a third label, slides were counterstained with 4'6-diamidino-2-phenylindole (DAPI, Sigma, Inc) and mounted in Vectashield (Vector, Inc).

Analysis of DECORE distribution: To demonstrate the distribution of DECORE immunoreactivity, we captured images of the E17 dorsomedial cortical wall in the FITC channel for Cx32 staining and the DAPI channel for the DAPI counterstain. We aligned composite images of Cx32 staining and DAPI counterstain to observe the distribution of cells with cytoplasmic Cx32 labeling with respect to the cytoarchitechtonic divisions of the cortical wall: the VZ, SVZ, IZ, SP, CP, and MZ.

Chapter 2

Expression of Connexins 26 and 32 during neocortical neurogenesis

A. Specificity of antibodies:

We performed immunoblot analyses on E14 and E17 forebrain tissue enriched for membrane proteins by alkali extraction, an established protocol for detection of connexins (Nadarajah, Jones et al. 1997; Mambetisaeva, Gire et al. 1999). Blots were probed with the same commercially produced affinity purified polyclonal antibodies we used for immunohistochemistry (Zymed #51-2800 for Cx26 and #71-0600 for Cx32). Results are shown in Figure 2.1. The anti Cx26 antibody labels a single band at approximately 24kD in both adult liver and forebrain at E14 and E17, consistent with previous studies. It is well described in the literature that Cx26 and Cx32 both migrate at a slightly lower mass than expected from their predicted amino acid sequences.

The anti Cx32 antibody labels a band at approximately 27 kD in E17 forebrain and adult liver, corresponding to the monomeric form of Cx32. Additional bands are seen around 55 and 85 kd, intervals consistent with dimers and trimers of Cx32. The predominant band for E14 is at 55kD. To ascertain that these higher molecular weight bands represent Cx32, we incubated replicas of the blots for E17 forebrain and adult liver with the same antibody pre-adsorbed to the blocking peptide, the Cx32 peptide fragment used to generate the antibody. As shown in Figure 2.1D, none of the bands are recognized in forebrain or liver by the specifically pre-blocked antibody. One band at around 40kD is faintly labeled in E17 forebrain, but this band is not normally labeled in the absence of the blocking peptide.

It is therefore apparent that our Cx32 antibody is specific to Cx32 and recognizes different forms of the protein. The most parsimonious explanation is that these different forms of Cx32 are in fact multimers, as is frequently observed with connexins separated by SDS/PAGE. The presence of monomeric vs. multimeric forms is likely an artifact of proteins under denaturing conditions.

Figure 2.1. Western blot analysis showing specificity of anti-connexin antibodies. All blots shown were taken from 8-16% gradient SDS PAGE gels transferred to nitrocellulose and probed as described.. Equal quantities of protein (approximately 100ug) were loaded into each lane. **A**. Immunoblots of E14 forebrain probed with anti-Cx26 (left lane) and anti-Cx32 (right lane). Cx26 is present as a single band at approximately 24 kD, characteristic of the monomeric form. Cx32 is recognized primarily in bands whose molecular weights correspond to dimers and. 3-mers of the protein. **B**. Imunoblots of E17 forebrain. Cx26 is again recognized as a single band at approximately 24 kD. Cx32 is labeled in its monomeric form (band at approximately 27 kD) and as a 3-mer (upper band). **C**. Immunoblots of adult liver. the positive controls for both the Cx26 and Cx32 antibodies. Each antibody specifically recognizes its respective monomer. The Cx32 antibody also labels the dimeric form. **D.** Negative controls for the specificity of anti-Cx32; Immunoblot of E17 forebrain (left lane) and adult liver (right lane) probed with anti-Cx32 antibody pre-adsorbed with the blocking peptide. The blocking peptide prevents labeling of all bands seen in A., B., and C. One residual non-specific band is labeled at approximately 33 kD in E17 forebrain.

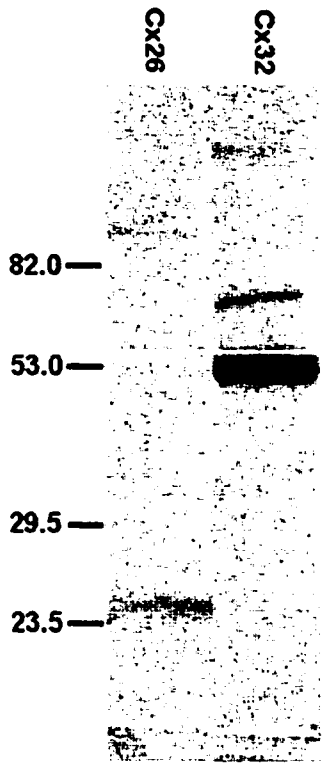

A. E14 Forebrain

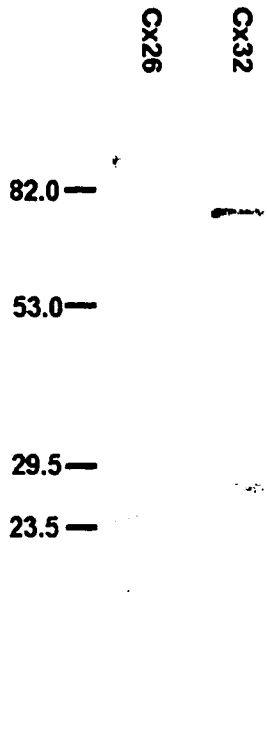

B. E17 Forebrain

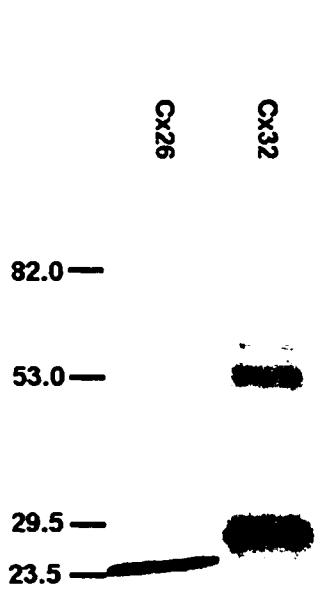

C. Adult Liver

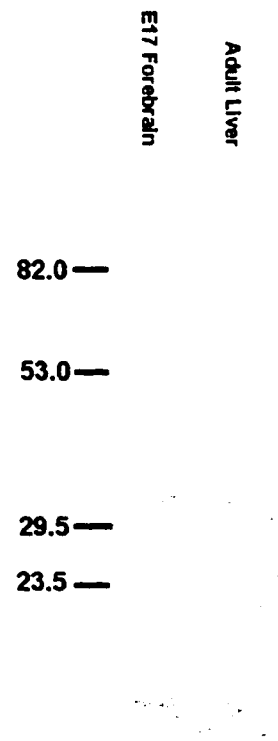

D. Cx32 Block

To ascertain the specificity of the Cx32 antibody for immunohistochemistry, we preadsorbed it with the blocking peptide prior to immunostaining sections of E17 neocortex. As shown in Figure 2.2, this resulted in an almost complete block of immunostaining.

Certain lots of the anti Cx32 antibody displayed a unique pattern of immunostaining in which a subpopulation of cells in the neocortex were labeled around and perhaps in, the nucleus (see Chapter 4). This pattern was seen exclusively in the cortex and only at later embryonic stages. Since we also found this pattern in Cx32 null mice, it is unlikely that it represents Cx32 expression. As described in Chapter 3, we exploited the cross reactivity of this particular lot of antibody to isolate a novel cortex-specific protein. At earlier stages, both immunoblots and immunohistochemistry showed identical results with all lots of antibody used (results not shown). All lots of Cx32 antibody recognized Cx32. But for later stages, we used only the lots of antibody that did not show the cross-reactivity.

B. Cx26 and Cx32 are expressed in the embryonic neocortex throughout neurogenesis

As stated above, the primary aim of our initial study was to survey the expression patterns of Cx26 and Cx32 in the context of predominant developmental events during neocortical neurogenesis: cell proliferation, neuronal migration, and differentiation. The embryonic ages we analyzed spanned neocortical neurogenesis from its inception at E12 to its culmination at E17. For each stage, we performed immunostaining for Cx26 and Cx32 in conjunction with Tuj1, a neuronal marker. In addition, we performed BrdU labeling studies at mid and late neurogenesis to mark cells in S-phase of the cell cycle. Together, these analyses allowed us to visualize relationships between Cx26 and Cx32 expression and concurrent developmental events.

Expression at E12, early neurogenesis: At E12, punctate immunoreactivity for both Cx26 and Cx32 is seen throughout the cortical wall (Figure 2.3 B, C). This punctate pattern has been classically observed for connexin immunostaining and is thought to label

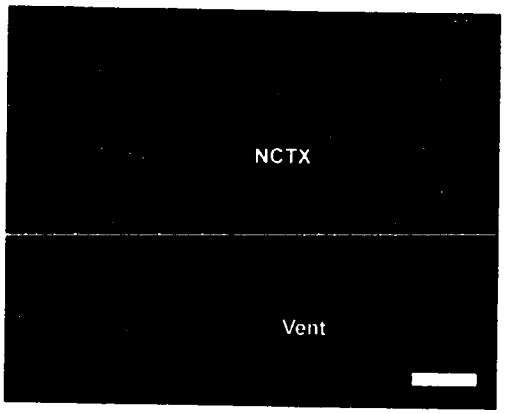

A. E17 Cx32

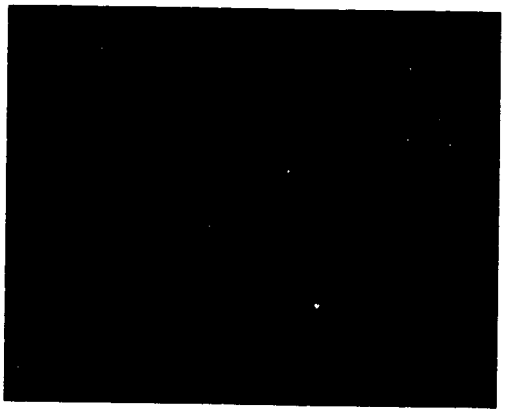

A. E17 Cx32 Blocking Peptide

Figure 2.2. Specificity of anti-Cx32 antibody in immunohistochemical staining (**A**) Sections of E17 forebrain immunolabeled with anti-Cx32. Dorsal surface is up. NCTX=neocortex, V=ventricle. Scale bar=100um. (**B**) Immunostaining with anti-Cx32 pre-incubated with the blocking peptide. The blocking peptide largely eliminates the immunostaining seen in A.

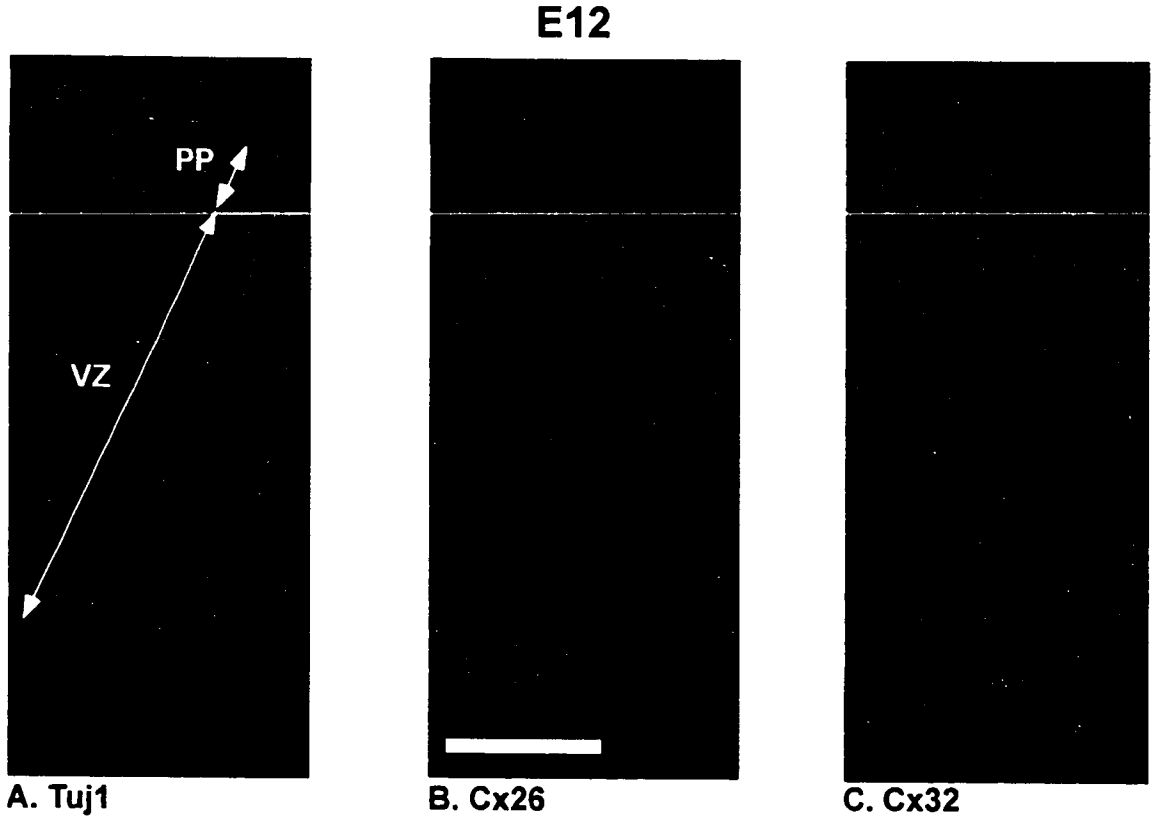

Figure 2.3. Neuron-specific tubulin (Tuj1), Cx26, and Cx32 immunolabeling at E12, early in cortical neurogenesis. All immunostaining was performed in adjacent coronal sections of the same brain. Scale bar = 50uM. In this and all subsequent figures, ventricular surface is facing down unless otherwise noted. Cx26 (**B**) and Cx32 (**C**) both show a classic punctate staining pattern that is mostly overlapping and uniform through the thickness of the cortex. (**A**) Immunostaining for Tuj1 delineates the pre-plate (PP; Tuj1 labeled neurons near the pial surface) and ventricular zone (VZ; cells unlabeled by Tuj1). Note that Tuj1 labeled neurons in the PP and proliferative cells in the VZ each express both Cx26 and Cx32.

membrane gap junction channel assemblies at points of coupling between cells (Li, Hertzberg et al. 1997; Nagy, Ochalski et al. 1997). We thus designate this punctate pattern as *membrane* immunoreactivity. At E12 and later stages, immunostaining for Cx32 is more robust than for Cx26. Although it could reflect higher expression levels for Cx32, this disparity could also arise from differences in the relative affinities of the antibodies. For this reason, we do not interpret relative levels Cx26 and Cx32 immunoreactivity in a strict quantitative sense. We focus instead on comparisons of Cx26 and Cx32 expression in terms of their temporal and spatial patterns.

Immunostaining for the neuronal marker Tuj1 (Figure 2.3A) in an adjacent section reveals the corresponding pattern of neuronal differentiation across the cortical wall. Cells unstained by Tuj1 comprise the proliferative cells of the ventricular zone (VZ) (Boulder Committee 1970) while Tuj1 stained cells at the pial surface represent the early differentiated neurons of the preplate (PP) (Menezes and Luskin 1994). Cx26 and Cx32 both show membrane immunoreactivity in the VZ (Figure 2.3 B,C) and PP. Cx32 immunostaining appears uniform between the two zones. Cx26 expression, however, is more robust in the PP than in the VZ.

Expression at E14, mid neurogenesis: E14.5 marks the midway point of neocortical neurogenesis. At this time, equal numbers of cells are leaving and reentering the cell cycle (Takahashi, Nowakowski et al. 1996). Tuj1 immunostaining at E14 (Figure 2.4A) shows increased numbers of neurons present within a distinct intermediate zone (IZ), cortical plate (CP), and marginal zone (MZ). At the same time, cells unstained by Tuj1 delineate a VZ at its maximum size—as neurogenesis proceeds, an increasing proportion of cells exit the cell cycle and migrate out of the VZ toward the CP. Cells in S-phase of the cell cycle were labeled by BrdU uptake after a 45-minute survival time (Figure 2.4A, inset). The majority of cells in S-phase occupy a distinct region in the outer aspect of the VZ, reflecting the classically observed pattern for interkinetic nuclear migration (Takahashi, Nowakowski et al. 1992; Takahashi, Nowakowski et al. 1993). A small number of BrdU labeled cells are found at the VZ/IZ border,

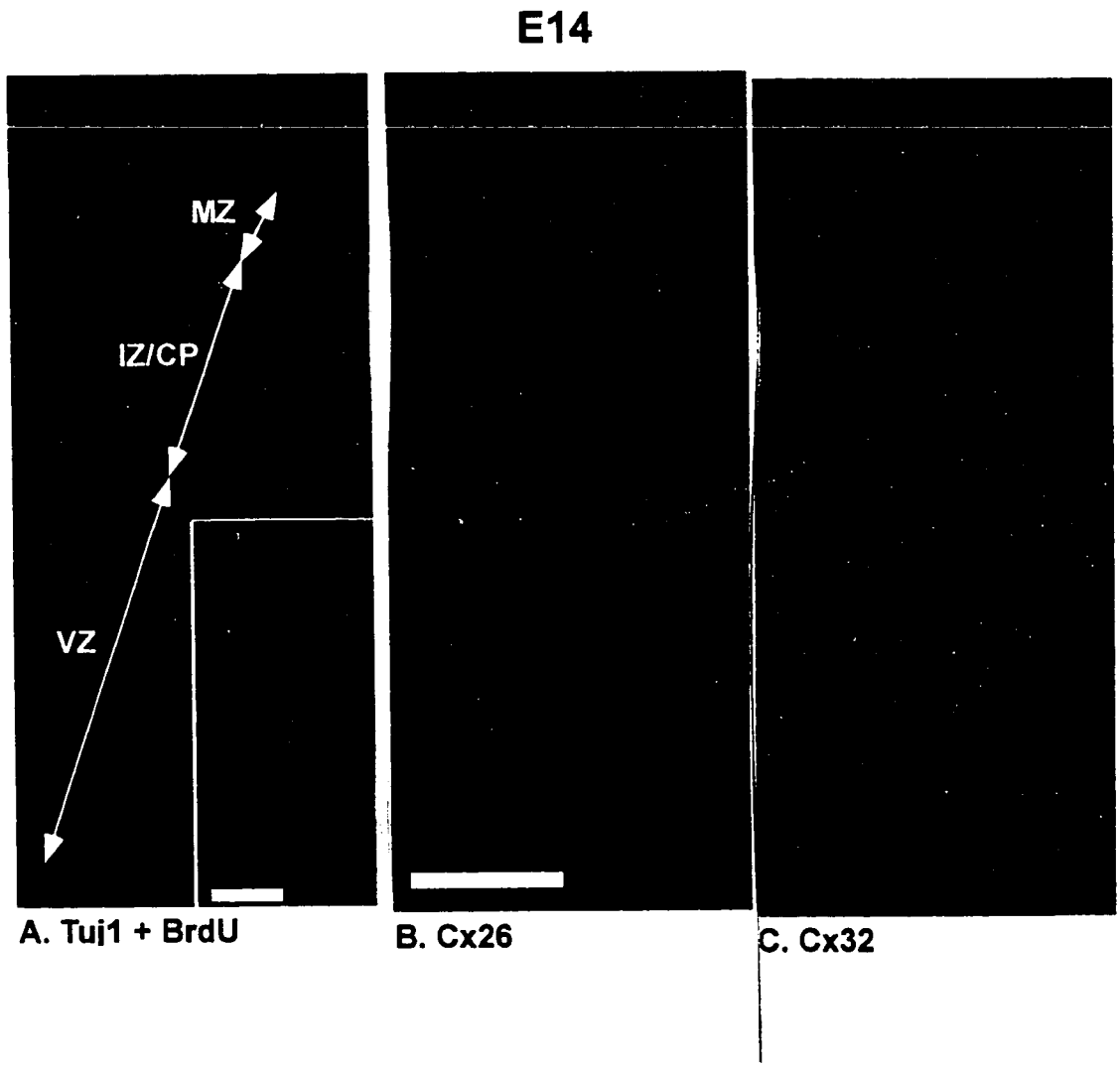

Figure 2.4. Tuj1, BrdU, Cx26, and Cx32 immunolabeling at E14, mid neurogenesis. All scale bars =50 uM. Tuj1 staining at E14 (**A**) is more extensive than at E12, showing a distinct marginal zone (MZ) and a rudimentary intermediate zone (IZ) and cortical plate (CP). BrdU/Tuj1 double labeling demonstrates that cells in S-phase (encompassing the upper portion of the VZ) are distinct from the Tuj1 labeled population. Note that regions with proliferating, migrating, and differentiating neurons (the VZ, IZ/CP, and MZ) show punctate membrane immunoreactivity for both Cx26 (**B**) and Cx32 (**C**).

corresponding to a previously described secondary proliferative population (Takahashi, Nowakowski et al. 1994). As expected, no neurons (Tuj1 labeled cells) are BrdU labeled. Cx26 and Cx32 show apparently uniform membrane immunoreactivity across the major cytoarchitechtonic divisions: the VZ, IZ, CP and MZ (Figure 2.4B,C). Aside from a slight concentration of membrane immunoreactivity in mitotic cells at the ventricular surface, there is no apparent difference in Cx26 or Cx32 immunoreactivity between cells in the outer VZ (where most BrdU labeled S-phase cells are located) and cells in the VZ at other stages of the cell cycle. Therefore, Cx26 and Cx32 membrane immunoreactivity is maintained by proliferative cells throughout the cell cycle and by neurons in the IZ, CP, and MZ.

Expression at E16, late neurogenesis: Tuj1 staining at E16 (Figure 2.5A) shows a substantial expansion of the CP and the appearance of a subplate (SP) and subventricular zone (SVZ). Conversely, the size of the VZ has decreased considerably, reflecting a reduced rate of proliferation. At this time, the CP is composed primarily of neurons that have migrated to form the deeper cortical layers, IV and V (McConnell 1995; Polleux, Dehay et al. 1997; Takahashi, Goto et al. 1999). BrdU labeling after a 30-minute survival time (Figure 2.5B) reveals a population of cells in S-phase encompassing a large portion of the VZ. Another population of BrdU labeled cells, likely glial precursors (Takahashi, Nowakowski et al. 1994), is scattered throughout the SVZ. Again, membrane immunoreactivity is seen for both Cx26 and Cx32 in proliferative (VZ and SVZ), migrating (IZ), and post-mitotic (Tuj1 labeled) cells. Moreover, cells in S-phase show similar patterns of Cx26 and Cx32 labeling as other cells in the VZ, at other stages of the cell cycle.

Expression at E17, the final day of neocortical neurogenesis: At E17, the cortical plate occupies an increasingly large portion of the cortical wall (Fig.1-6A, Tuj1 labeling). The VZ, in contrast, has regressed to an area limited mostly to the ventricular surface, as is evident from the locations of BrdU labeled cells in S-phase (30 minute survival time; Figure 2.6B).

Figure 2.5. Tuj1, BrdU, Cx26, and Cx32 immunolabeling at E16, late neurogenesis. Scale bar=50uM. Cx26 and Cx32 both continue to show uniform membrane immunoreactivity through the cortical wall. Tuj1 labeling (**C**) demonstrates the extent to which differentiated neurons are present throughout the cortical wall, while the VZ represents a smaller fraction of the cortical thickness. Tuj1/BrdU double labeling (**B**) reveals S-phase cells in the VZ and subventricular zone (SVZ), the likely site of later cortical glial genesis. These areas containing proliferating cells in S-phase (BrdU labeled cells) also show membrane immunoreactivity for both Cx26 and Cx32.

E16

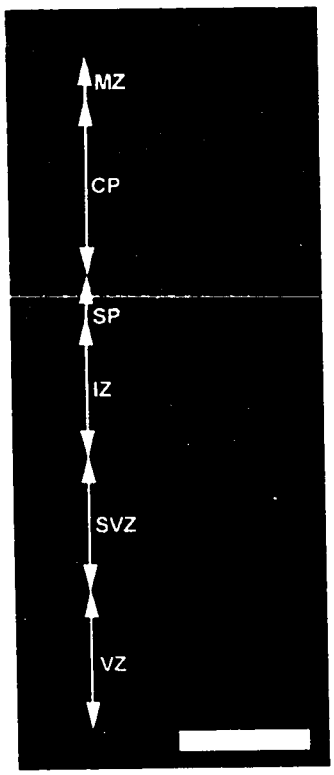

A. Tuj1

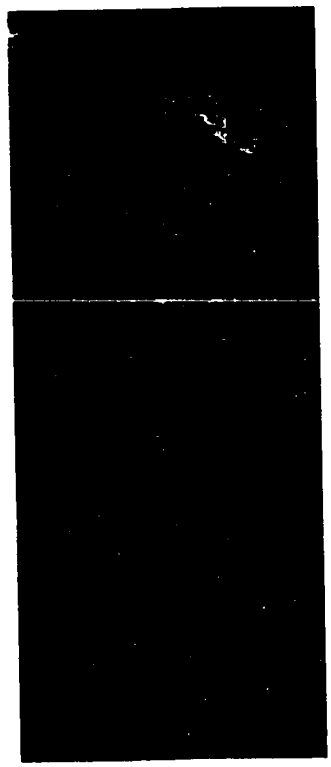

B. Tuj1 + BrdU

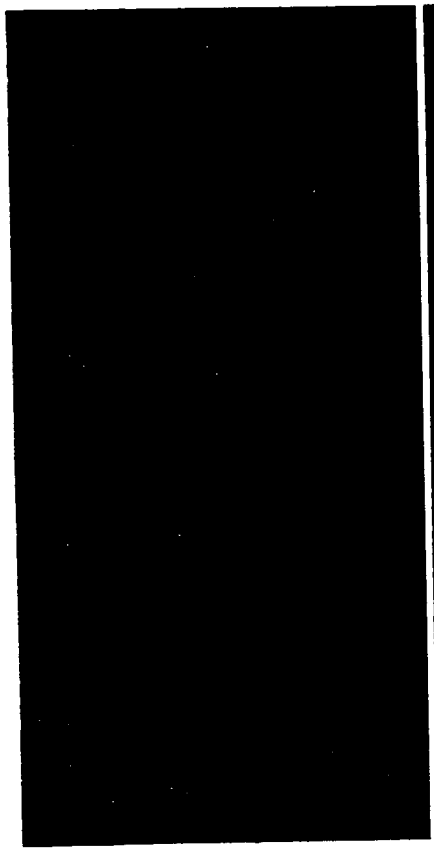

:. Cx26

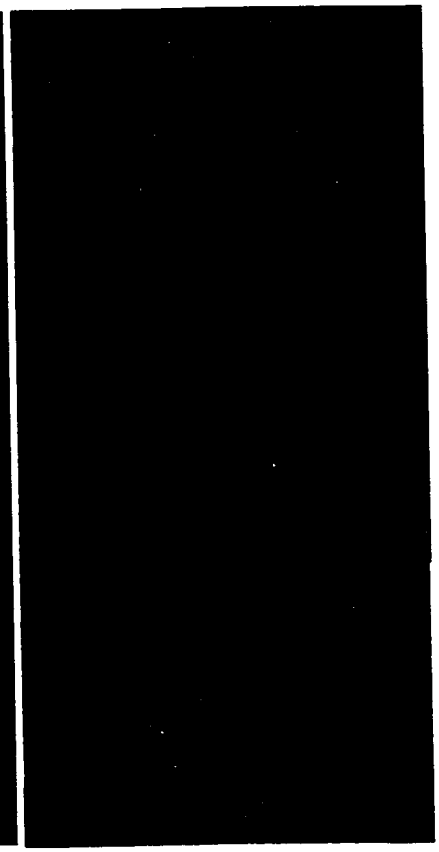

D. Cx32

Figure 2.6. Tuj1, BrdU, Cx26, and Cx32 immunolabeling at E17, the final day of neocortical neurogenesis. All scale bars=50 uM. Tuj1 labeling (**A**) shows a more extensive CP, IZ, and SVZ while the VZ is vestigial. Tuj1/BrdU labeling (**B**) reveals a larger population of S-phase cells comprising the SVZ. Cx26 (**C**) and Cx32 (**D**) now show apparent differences in expression pattern with decreased intensity of Cx26 immunostaining though the IZ, SP, and lower CP.

E17

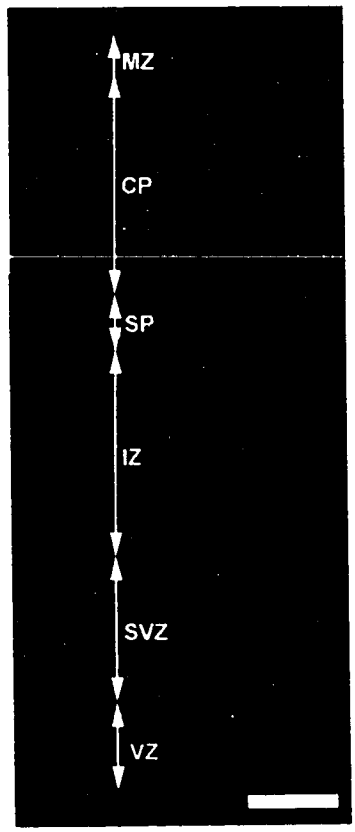

A. Tuj1

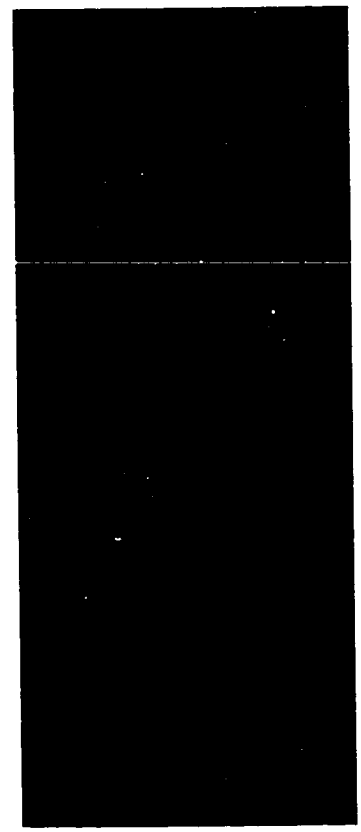

B. Tuj1 + BrdU

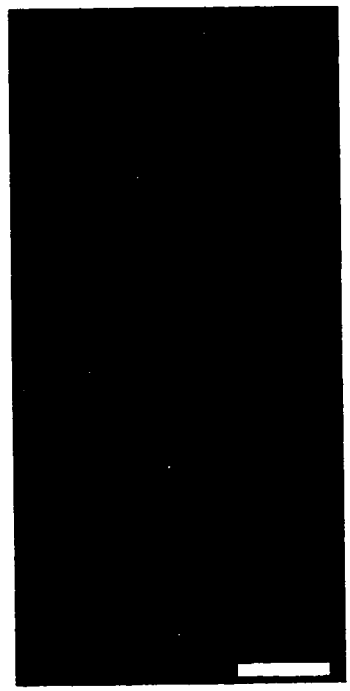

C. Cx26

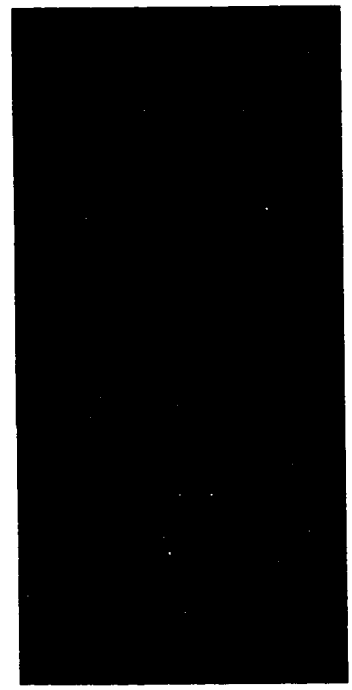

D. Cx32

Proliferation of neuronal precursors has slowed markedly and there is a massive migration through the IZ of neurons destined to occupy layers II/III (Gadisseux, Evrard et al. 1992). At the same time, increasing numbers of BrdU labeled cells occupy the SVZ, reflecting an increased rate of glial production (Caviness).

At this stage, Cx26 and Cx32 show a dramatic divergence in expression patterns. Cx26 continues to show uniform membrane expression throughout the VZ/SVZ and CP. However, in the intervening IZ, Cx26 expression is conspicuously decreased. Cx32 expression remains relatively uniform throughout the cortical wall, aside from an apparent decrease in immunolabeling around the SP.

C.). Cx26 and Cx32 show variable expression between proliferating,migrating, and differentiated cell populations at different times during neurogenesis

The membrane expression patterns we observed for Cx26 and Cx32 in the neocortex at all embryonic ages left us with the following questions: 1. Do either Cx26 or Cx32 show a significant variation in expression level between different cell populations within different cytoarchitectonic divisions of the neocortex (i.e., proliferating, migrating, and differentiating neurons contained within the VZ, IZ, and CP, respectively)? 2.Within each of these areas, is there a significant difference between expression levels of Cx26 and Cx32?

We performed a series of image analyses to quantitatively compare the spatial distributions of Cx26 and Cx32 across the cortical wall. Composite images of adjacent Cx26 and Cx32 fluorescent immunostained sections of the cerebral wall were converted to a 0 to 255 grayscale and inverted using Scion Image software (Scion, Inc.). The sections were divided into 10 bins whose height was 10% of the ventricular to pial distance and whose width was 100uM for E12-E16 and 200uM for E17. The average gray value was measured for each bin, again using Scion Image. In these analyses, we compared patterns of Cx26 and Cx32 membrane immunoreactivity in adjacent sections at E12 (n=5 brains from 3 litters), E14 (n=6 brains from 3 litters), E16 (n=5 brains from 2

litters), and E17 (n=6 brains from 4 litters). Examples of analyzed images are shown in Figures 2.7A, 2.8A, 2.9A, and 2.10A.

We analyzed the data in two ways to address each of the questions presented above. To address our first question of whether Cx26 or Cx32 show differences in expression relating to developmental processes, we measured individual expression patterns of Cx26 and Cx32 across the cortical wall as described above. We then grouped bins for each connexin at each age into categories of proliferative regions (Pro), regions consisting predominantly of migrating neurons (Mig), and those containing mostly differentiated neurons (Dif.). Pro regions encompassed the VZ and at later stages, the SVZ. Mig regions included only the (well defined) IZ and were therefore designated only at E16 and E17. Dif regions included the CP (PP at E12), along with the SP and MZ at later stages. These designations were different for each age to reflect developmental changes in the sizes of each cytoarchitectonic division. For E12, Pro=bins 1-8 and Dif=bins 9 and 10; for E14, Pro=bins 1-6 and Dif=bins 7-10; For E16, Pro= bins 1-4, Mig=bins 5-6, and Dif=bins 7-10; for E17, Pro=bins 1-2, Mig=bins 3-5, and Dif=bins 6-10. For each connexin at each age, we grouped results of all brains analyzed and performed a one way analysis of variance (ANOVA) to determine if there was a significant variation with respect to average gray values of Pro vs. Dif vs. Mig. (when present at E16 and E17). We defined significance as $P<.05$.

To address our second question of whether Cx26 and Cx32 show differences in expression patterns within different cell populations required that we analyze our data differently. As mentioned above, absolute differences in immunostaining intensity between Cx26 and Cx32 should not be interpreted quantitatively since these differences could arise from factors such as relative antibody affinity, that are not directly related to protein concentration. To overcome this limitation, we normalized the data for each Cx26 or Cx32 immunostained section such that the gray value in each bin is expressed as a proportion of the maximum gray value for the section. In this manner, we are able to compare Cx26 and Cx32 staining as a function of their relative intensities across the

cortical wall, between Pro, Mig, and Dif populations. At each age, we grouped normalized values for each connexin into Pro, Mig, or Dif designations as described above. We then compared normalized Cx26 and Cx32 values within Pro, Mig, or Dif populations using a two-tailed t-test.

The results of our analyses are shown in Figures 2.7, 2.8, 2.9,and 2.10 for E12, E14, E16, and E17, respectively. Our analyses regarding individual variation of Cx26 and Cx32 across different cell populations in the cortical wall are shown in parts A and B of each figure. Data for each stage are shown for each connexin in plots of average gray value Vs cortical bin (1-10). Each data point represents a gray value measurement for one brain for the specified bin. The plots and corresponding examples of analyzed images are labeled with respect to the grouping of cortical bins we designated as belonging to Pro, Mig, or Dif cell populations. Results of our analyses comparing Cx26 and Cx32 patterns of immunoreactivity are shown in part C of each figure.

One remarkable feature of the data for each connexin at each stage is the extent to which average gray values for each bin are consistent between brains. The range of gray values for each bin at a given stage were typically less than 50 gray value points on a 0 to 255 scale; less than 20% variation across the possible range. Another common feature of the data between stages was that when gray values of connexin immunostaining were normalized for each section to the bin with the maximum gray value, the highest normalized values (at or near 1) were most often in bin 10. At all stages we analyzed, bin 10 corresponded to the Dif population. Whether Cx26 or Cx32 showed significant differences in imunoreactivity across different cell populations, varied by stage. Likewise, different stages showed variable results with respect to comparisons of normalized staining patterns for Cx26 and Cx32.

For E12, analyses by one way ANOVA revealed variation between Pro and Dif populations that was significant for Cx26, but not for Cx32. These results reflect differences that are readily apparent in the corresponding sample images.

Figure 2.7 Analysis of Cx26 and Cx32 Immunoreactivity Patterns at E12: Digital Images of E12 neocortex immunostained for Cx26 or Cx32 were converted to grayscale, inverted, and divided into bins as described. Samples of the images analyzed for the respective connexins are shown to left of the graphs in A and B Note the arrows in A indicating the cytoarcitechtonic regions and the corresponding designations (Pro or Dif) used for analysis. For each brain used (N=5 from 2 litters), adjacent sections were stained for Cx26 and Cx32 and analyzed. One section per brain was used for analysis. Graphs in A and B display the compiled data for Cx26 and Cx32, respectively. Each data point represents the average gray value on a 0 to 255 scale for one brain in the designated bin. Note the tight grouping of data points relative to the range of possible values. The broken lines indicate the demarcation of the bins into Pro or Dif populations. For both Cx26 andCx32, Pro and Dif data were compared by one-way ANOVA to determine if variation in values between Pro and Dif groups was greater than the variation within each population and hence, statistically significant. Significance is defined at the $P<.05$ level. P-value for Cx26 data (A) = .005. Therefore, differences in Cx26 immunoreactivity between Pro and Dif populations are significant. For Cx32, the immunoreactivity pattern is not significant; P=.956. **Part C.** summarizes comparisons between Cx26 and Cx32 immunoreactivity patterns, normalized for each brain as described in the text. With this normalization, the maximum bin value within a section stained for Cx26 or Cx32 is 1 and the other bin values within that section are expressed as a fraction thereof. The graph on the left displays the mean normalized values for each bin across the cortical wall for both Cx26 and Cx32. Error bars denote SEM. Note the larger differences between Cx26 and Cx32 in bins 1-4, within the Pro population. Cx26 data for bins within Pro populations were pooled and compared to those of Cx32 using a two-tailed t-test. The same analysis was used to compare normalized Cx26 and Cx32 values in Pro regions. The bar graph on the right summarizes this analysis, showing the means for.Cx26 and Cx32 in Pro and Dif groups. Error bars show SEM and asterisk above denotes a statistically significant difference ($P<.05$) by t-test. The normalized immunoreactivity pattterns are significantly different for Cx26 and Cx32 within the Pro population (P.002), but not the Dif. (P=.105). As we describe in the text, non-significant differences between Cx26 and Cx32 expression patterns implies a greater probability of Cx26/32 heteromeric channels within that region.

E12

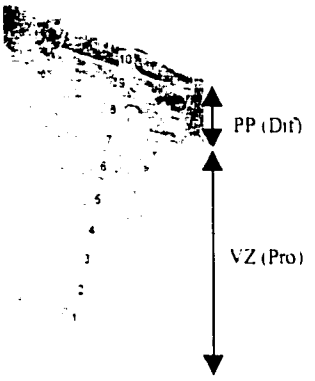

A. Cx26

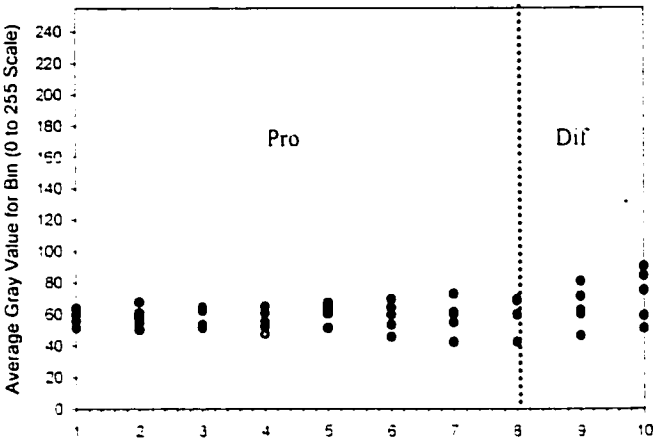

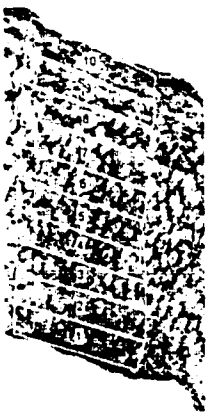

B. Cx32

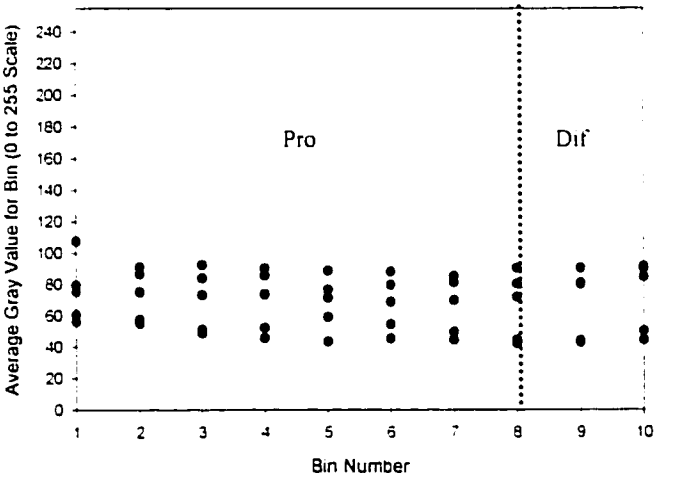

C. Comparison of Normalized Cx26 and Cx32 Immunoreactivity Patterns

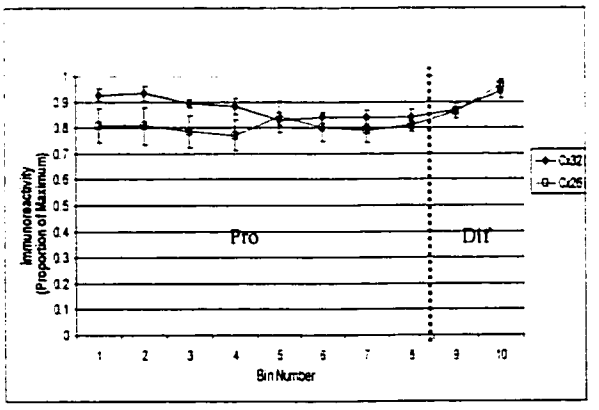

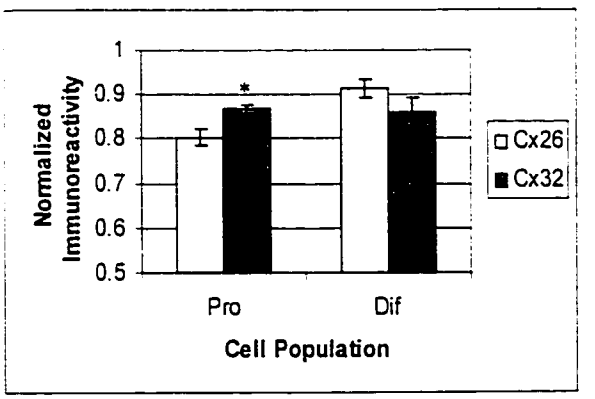

Figure 2.8 Analysis of Cx26 and Cx32 Immunoreactivity Patterns at E14: The format of this figure is the same as that of Figure 2-7 (see figure legend for description). Cx26 (A) and Cx32 (B) show similar expression patterns across the cortical wall. By one-way ANOVA, both Cx26 and Cx32 show significant differences in immunostaining intensity between Pro and Dif populations (for Cx26, P=.02; for Cx32 P=.003). Comparisons of normalized Cx26 and Cx32 immunoreactivity patterns via two-tailed t-test (summarized in C) reveal significant differences between the two connexins in pro ($P=2.52 \times 10^{-6}$) and Dif ($P=9.56 \times 10^{-5}$) populations.

E14

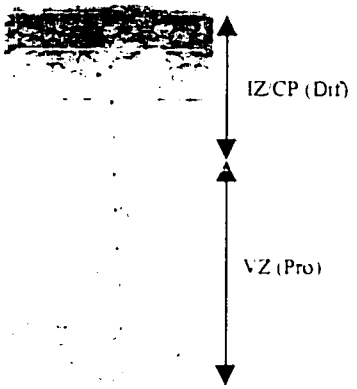

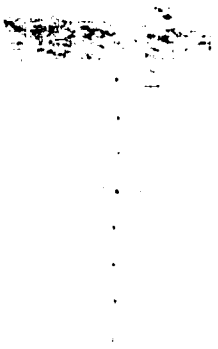

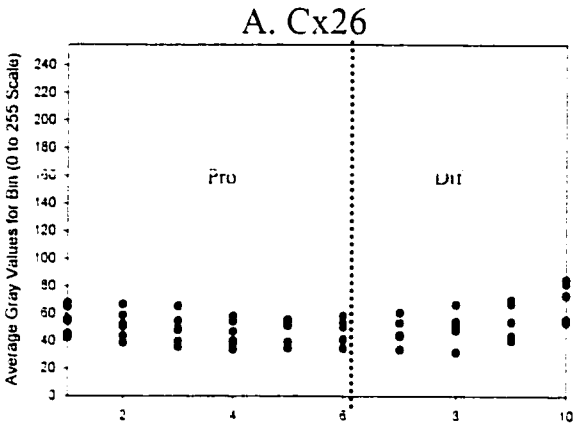

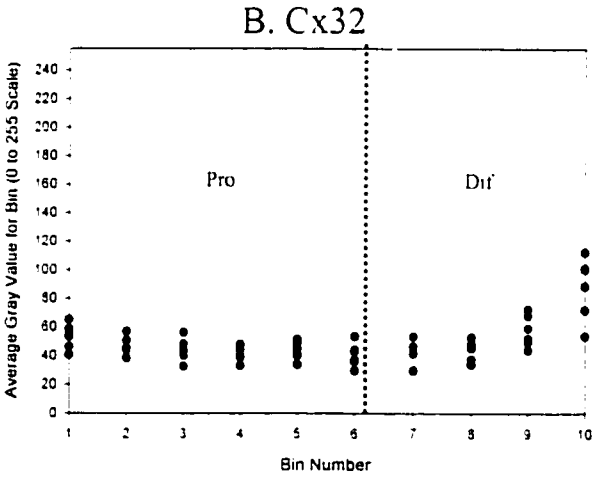

C. Comparison of Normalized Cx26 and Cx32 Immunoreactivity Patterns

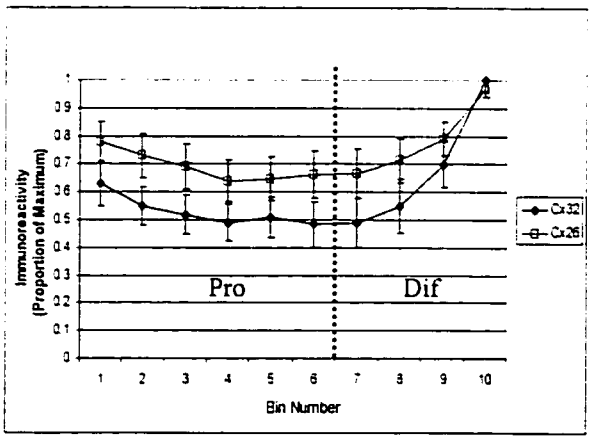

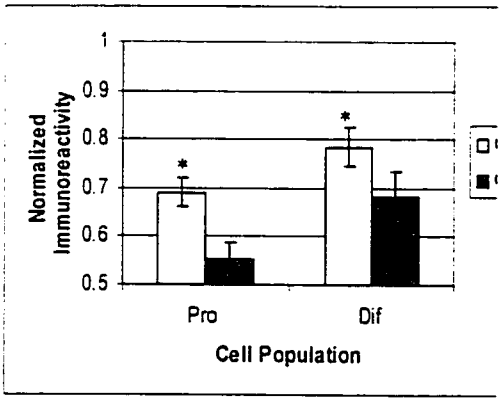

Figure 2.9 Analysis of Cx26 and Cx32 Immunoreactivity Patterns at E16: The format of this figure is the same as that of Figure 2-7 (see figure legend for description). Cx26 (A) and Cx32 (B) both show very uniform expression patterns across the cortical wall, that overlap to a large degree. By one-way ANOVA, neither Cx26 nor Cx32 show significant differences in immunostaining intensity between Pro and Dif populations (for Cx26, P=.727; for Cx32, P=.466). Comparisons of normalized Cx26 and Cx32 immunoreactivity patterns via two-tailed t-test (summarized in C) attest to their overlap: No significant differences are seen between Cx26 and Cx32 in Pro, Mig, or Dif populations.

E16

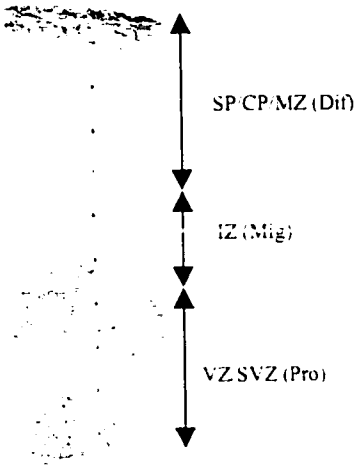

A. Cx26

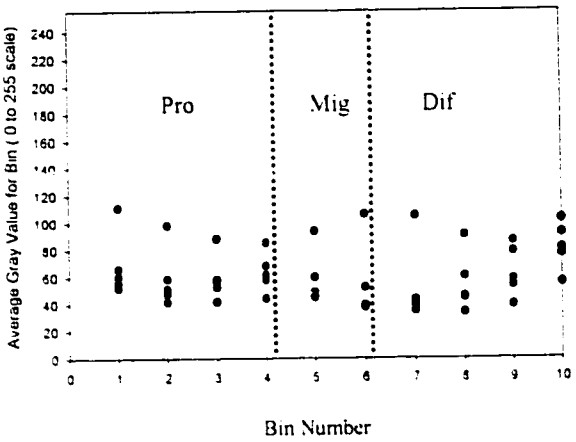

B. Cx32

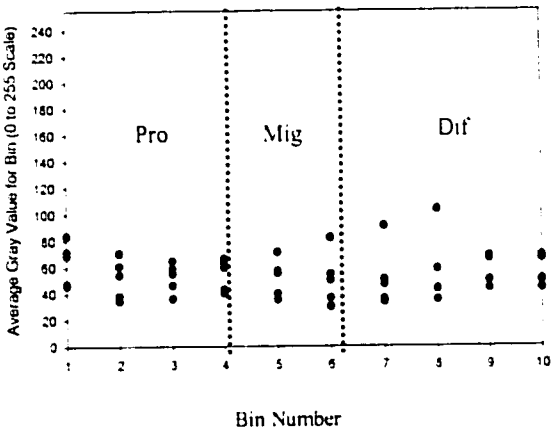

C. Comparison of Normalized Cx26 and Cx32 Immunoreactivity

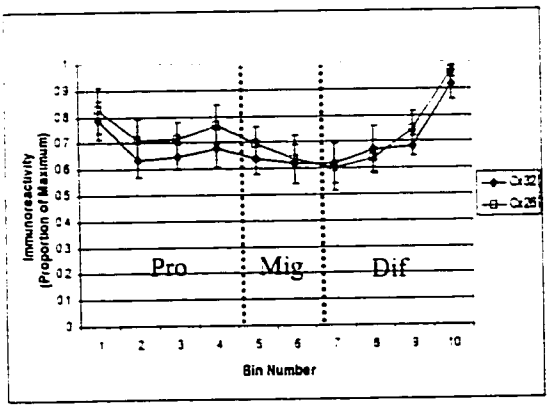

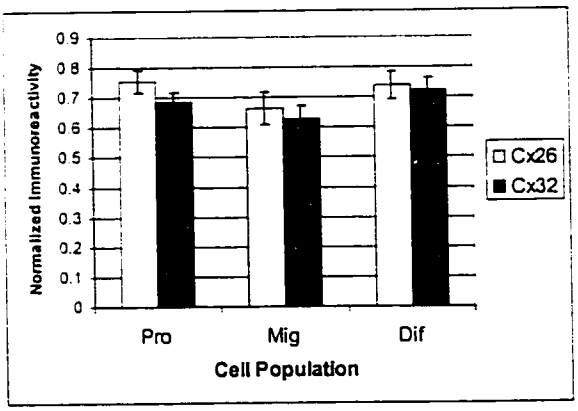

Figure 2.10 Analysis of Cx26 and Cx32 Immunoreactivity Patterns at E17: The format of this figure is the same as that of Figure 2-7 (see figure legend for description). Differences in Cx26 and Cx32 expression patterns are very apparent at this stage. For Cx26 (A), there is a trend toward reduced immunoreactivity in bins 4-7, representing the IZ and lower CP. By one way ANOVA, Cx26 shows a significant variation between Pro, Mig, and Dif groups ($P=7.41 \times 10^{-5}$) In contrast, Cx32 continues to show relatively uniform immunostaining across the cortical wall, with non-significant variation between the three groups (P=0.242). Comparisons of normalized Cx26 and Cx32 immunoreactivity patterns via two-tailed t-test (summarized in C) show significant differences between the two connexins in all three groups. P=.016 for Pro, 3.35×10^{-5} for Mig, and 1.82×10^{-7} for Dif.

E17

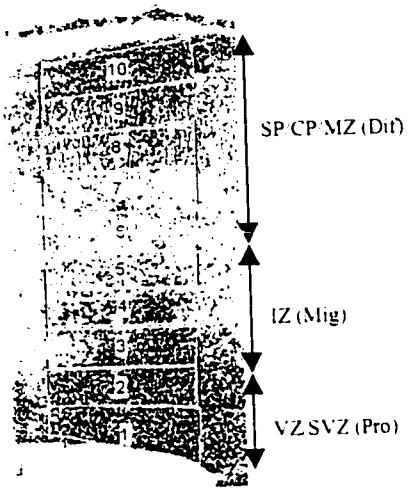

A. Cx26

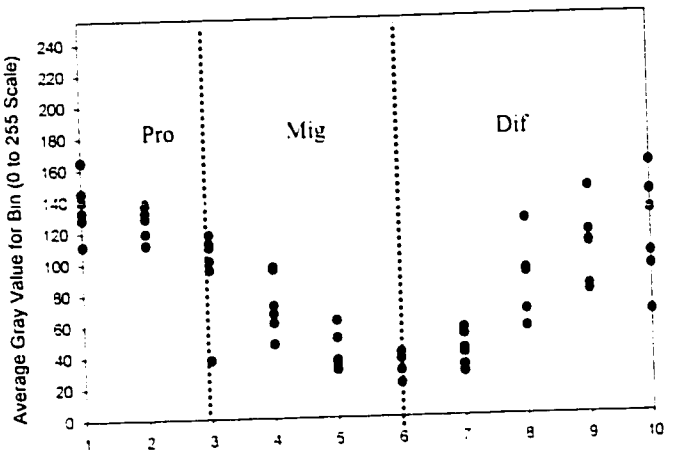

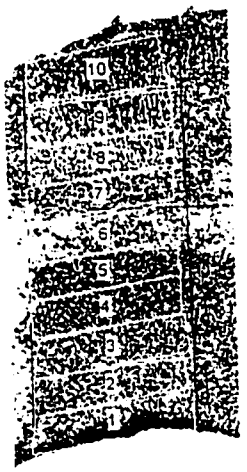

B. Cx32

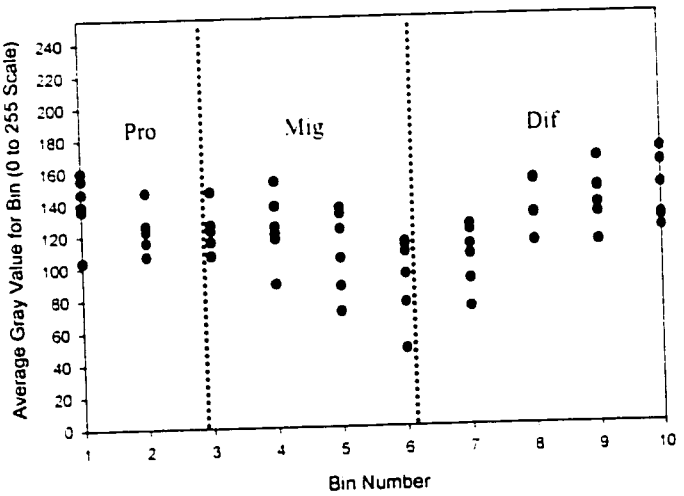

C. Comparison of Normalized Cx26 and Cx32 Immunoreactivity

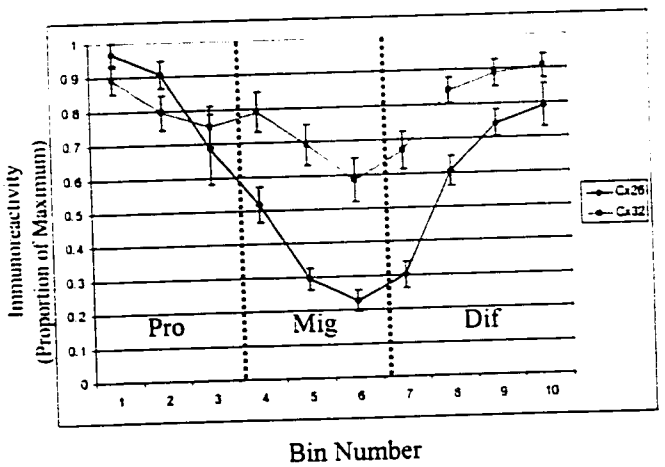

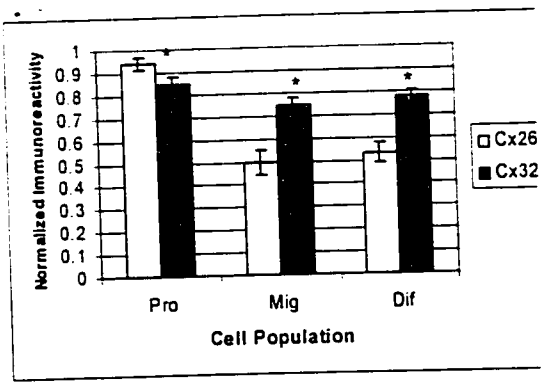

Immunoreactivity for Cx26 (Figure 2.7A) is noticeably more robust in the Dif area (comprised of the PP) relative to the rest of the section, while Cx32 immunoreactivity (Figure 2.7B) is by contrast, more uniform. Comparisons between normalized immunoreactivity patterns for Cx26 and Cx32 showed significantly higher relative expression for Cx32 among Pro cells (P=.002), but no significant differences between the two connexins among Dif cells(P=.105).

By visual inspection, E14 neocortex stained for Cx26 shows a very similar staining pattern to that seen for Cx32 (Figure 2.8A and B). Both Cx26 and Cx32 show significantly higher immunoreactivity among Dif cells than Pro cells (P=.02 for Cx26,P=.003 for Cx32). We note, however, that many migrating neurons are contained within the Dif population at E14, comprising bins 6-10. Within the Dif population, the highest immunoreactivity is clearly in the outer CP and MZ (bins 9-10). Comparisons of normalized immunoreactivity patterns at E14 (Figure 2.8 C) suggest a higher relative expression level for Cx26 in Pro cells ($P=2.52 \times 10^{-6}$), but a higher relative level of Cx32 expression in Dif cells ($P=9.56 \times 10^{-5}$).

Despite the appearance of an anatomically well-defined IZ at E16, immunostaining for both Cx26 and Cx32 appear more uniform than in preceding stages. Our analyses confirm this uniformity, showing no significant difference between Pro, Mig, and Dif. populations for either Cx26 or Cx32 (Figure 2.9 A and B; for Cx26, P=.727, for Cx32, P=.466). Cx26 and Cx32 show differences in relative immunoreactivity only among Pro cells, where Cx26 shows higher relative expression (P=.006).

The most striking feature of Cx26 immunostaining at E17 is the decrement of immunoreactivity in the IZ, SP, and lower CP (Figure 2.10A and B). Accordingly, our analyses indicate statistically significant variation of Cx26 immunoreactivity between Pro, Mig, and Dif Populations ($P=7.41 \times 10^{-5}$). In contrast, Cx32 displays comparatively uniform staining across the cortical wall, with no significant difference in immunoreactivity between these divisions (P=0.242). Among Pro cells, Cx26 shows

higher relative immunoreactivity (Figure 2.10 C; P=.016), while relative immunoreactivity is higher for Cx32 in Mig ($P=3.35 \times 10^{-5}$) and Dif ($P=1.82 \times 10^{-7}$) divisions. Our analyses at E17 suggest a down–regulation of Cx26 specifically among Mig cells in the IZ along with cells in the SP and lower CP.

Chapter 3
Neocortical development of the Cx32 null mouse

Our observation that Cx26 and Cx32 is expressed throughout neocortical neurogenesis in cells undergoing proliferation, migration, and differentiation suggests they may play a role in mediating these developmental processes. To investigate possible roles for Cx32, we examined neocortical development in Cx32 null embryos from a line generated by Dr. Klaus Willecke at Universitat Bonn. Although Cx26 mice have been generated, they are embryonic lethal at E10, two days before neocortical neurogenesis begins. We chose to focus on E17 since this stage represents a juncture between the end of neurogenesis and the start of processes, such as synaptogenesis, involved in the patterning of the adult neocortex. We received from Bonn, seven fixed E17 brains resulting from the mating of a heterozygous female and a hemizygous male (Cx32 is on the X chromosome). Of this litter, two were homozygous null, three were hemi/heterozygous, and two were wild-type, as revealed by PCR genotyping. To assess the degree to which normal development is altered in Cx32 null neocortex, we examined gross morphology and the expression of established immunological markers of neocortical development.

A. Cx32 null neocortex at E17 shows no gross differences in morphology when compared to hemi/heterozygous and wild-type littermates.

We examined gross morphology of the E17 brains by staining with Hematoxylin/Eosin (H&E) and a recently developed fluorescent Nissl stain (Neurotrace, Molecular Probes, Inc.). These stains individually or in combination, revealed the placement of cytoarchitectonic divisions of the cortical wall.

Results of H&E staining are shown in Figure 3.1. Differences in densities of cell bodies (dark blue/purple) and neuropil (pink/red) outline the ventricular/subventricular zone (VZ/SVZ), intermediate zone (IZ), subplate (SP), and cortical plate (CP). The

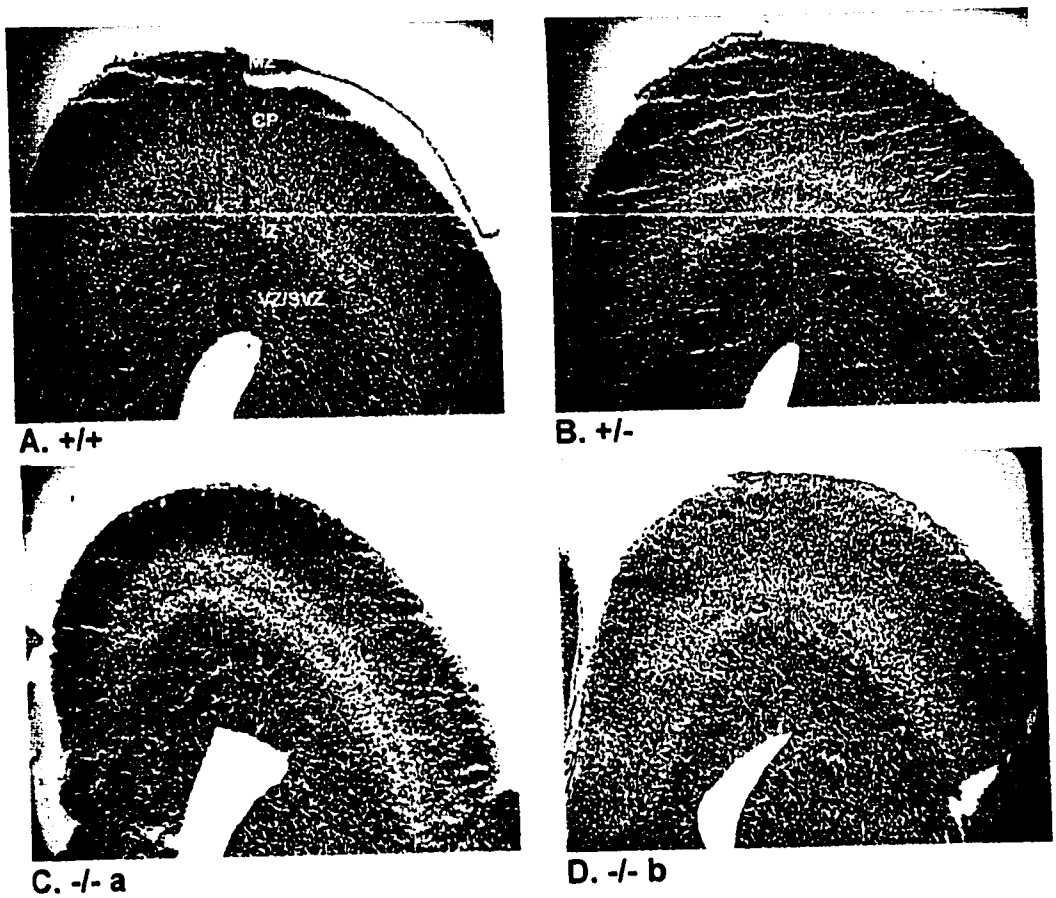

Figure 3.1. Histology of E17 Cx32 null neocortex: Hematoxylin/eosin stain. All sections are from brains taken form the same E17 litter. Genotypes are as labeled; sections from both of the two Cx32 null brains are shown. Pial surfaces are facing up; medial is left. Scale bar=100 uM. Arrows in A. correspond to the measurements we used for comparing relative areas of the cytoarchitectonic divisions shown in **Table 1.** VZ/SVZ=combined ventricular zone and overlying subventricular zone, IZ=intermediate zone, CP=cortical plate, MZ=marginal zone. Gap near the labeled MZ in A., with detached Pia Mater is a sectioning artifact. By visual inspection and quantitative comparisons, there does not appear to be altered gross morphology in Cx32 null neocortex.

placement of these divisions and their relative sizes are similar between Cx32 null brains and those of the hemi/heterozygotes and wild types. To ascertain this relationship in H&E stained sections shown, we performed measurements of cortical thickness in the ventricular to pial dimension and sizes of VZ/SVZ, IZ, CP, and MZ. The depth of each zone was divided by the total cortical thickness to reveal its percent contribution. The results are shown in Table 2-1 below. There are differences between genotypes with respect to percent contributions of each zone. However, the variability between the two Cx32 null brains (-/-a and -/-b) argues against any real effect.

Table 2-1. Results of measurements of sections in Figure 2-1. Values shown are percentages of cortical thickness (ventricular to pial dimension) represented by each of the specified cytoarchitectonic divisions of the cortical wall (rows) in wild-type, hemi/heterozygous, and Cx32 null brains (columns).

	+/+	+/-	-/-a	-/-b
VZ/SVZ	16	21	14	20
IZ	36	36	38	28
CP	43	39	43	46
MZ	3	4	4	4

Sections stained with fluorescent Nissl are shown in Figure 3.2.

The sections displayed are adjacent to the H&E stained sections in Figure 3.1. The zones demarcated by Nissl stain are equivalent to those revealed by H&E, but with better delineation of the fiber tracts running through the IZ. Nissl stain conveys essentially the same information as the H&E stain and further supports a lack of gross morphological defects in Cx32 null neocortex.

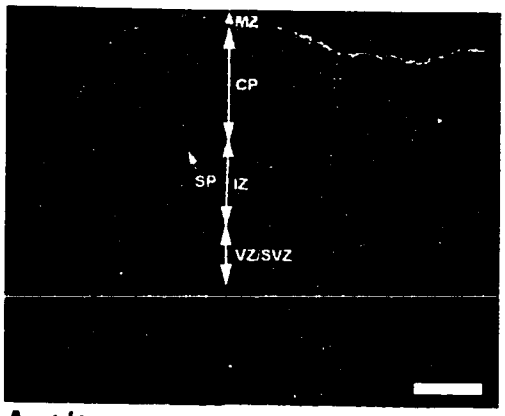

A. +/+

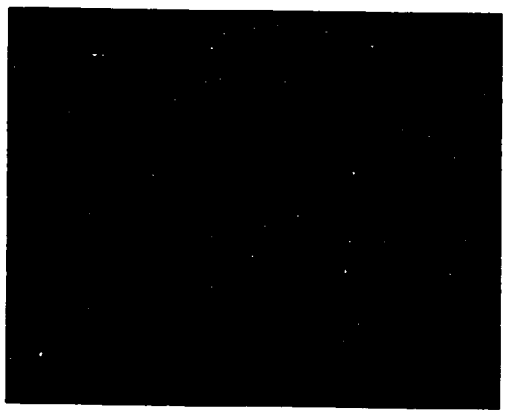

B. +/-

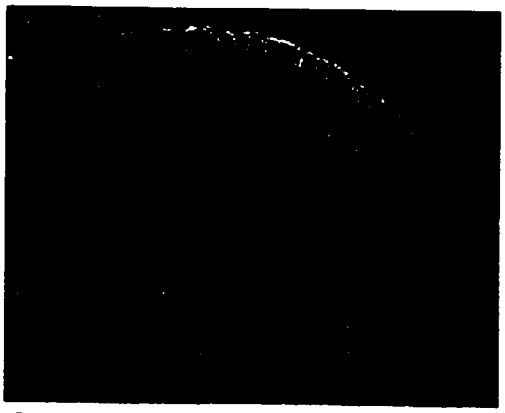

C. -/-

Figure 3.2. Histology of E17Cx32 null neocortex: Fluorescent Nissl stain. Pial surfaces are facing up; medial is left. Scale bar=100 uM. Arrows in A. denote the respective cytoarchitectonic divisions of the cortical wall. In this and all subsequent figures in this chapter, genotypes are as labeled in A., B., and C. Fluorescent Nissl stain conveys largely the same information as the histological stains shown in Figure 3.1, but with a better definition of fiber tracts.

B.Cx32 null neocortex shows no abnormalities in the expression of developmental markers

We performed immunohistochemical staining using established markers of neocortical development. Below we provide a brief description of these markers, our rationale for using them, and the results we obtained with each.

Tuj1: The Tuj1 antibody was originally generated by Frankfurter et.al. (cite) in a screen for neuron-specific markers in early embryos. The antigen recognized by Tuj1 is a form of class III Beta-Tubulin. In the previous results section, we used Tuj1staining in the early neocortex to differentiate the preplate/cortical plate from the VZ—the VZ is distinguished by its relative absence of Tuj1 staining. As seen in Figure 3.3, wild type, hemi/heterozygous, and Cx32 null neocortex sections stained for Tuj1 show similar sizes of rudimentary VZ. All three genotypes also contain sparsely distributed Tuj1 stained neurons in the VZ. A subpopulation of neurons are normally present in the VZ throughout neocortical neurogenesis, but are more prevalent later. These neurons have an interesting stellate morphology and are postulated by some authors to be tangentially migrating neurons (Menezes and Luskin 1994).

Because Tuj1 prominently labels neuronal processes, it can also function as a marker for developing fiber tracts. All three groups show a normal co-mingling of commisural axons and corticothalamic fibers in the medial IZ--the rudiments of what will constitute the white matter of the adult neocortex—and a divergence of these tracts as they move laterally.

Calretinin: Calretinin is a calcium binding protein that recognizes Cajal-Retzius cells along with other differentiated cell types in the developing neocortex and hippocampus. It has also been used historically as a neuroanatomical marker to delineate

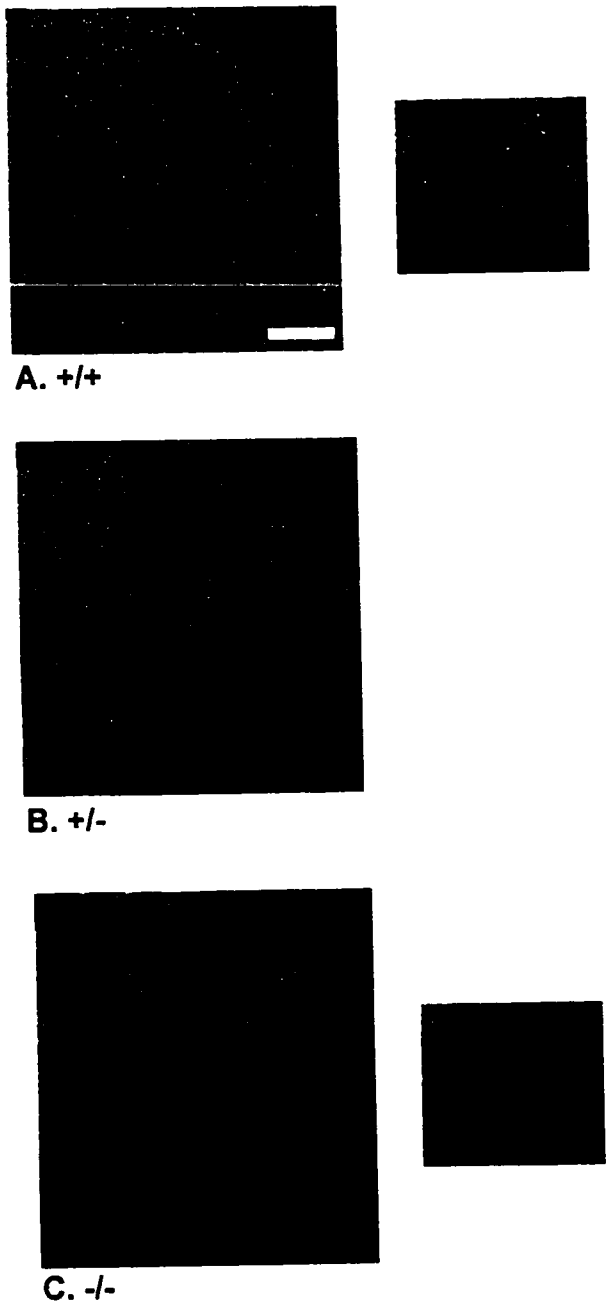

Figure 3.3. Immunostaining for neuronal marker Tuj1 in E17 Cx32 null neocortex. Pial surfaces are facing up; medial is left. Scale bar=100 uM. Tuj1 staining reveals the morphology of differentiated neurons and their processes. A subpopulation of Tuj1 labeled neurons are in the VZ of all three genotypes. These neurons are shown magnified in images to the right of A. and C. No apparent differences can be seen between +/+, +/-, and -/- neocortices. Discrepancies in the sizes and shapes of ventricles are due to slight differences with respect to the sectioning plane.

Figure 3.4. Calretinin immunostaining in E17 Cx32 null neocortex. Pial surfaces are facing up; medial is left. Scale bar=100 uM in A., B., and C. Scale bar=50uM in D. and E. In all three genotypes (in A., B., and C.), calretinin prominently labels thalamocortical axons and their presumptive terminals in the subplate. A high density of labeled cells are found medially and a smaller number occur more laterally in the CP. D. and E. show calretinin labeling of Cajal-Retzius cells in the MZ (arrows) of +/- and -/- neocortex, respectively. The DAPI counterstain reveals that densities of Cajal- Retzius cells are comparable between +/- and -/- neocortex.

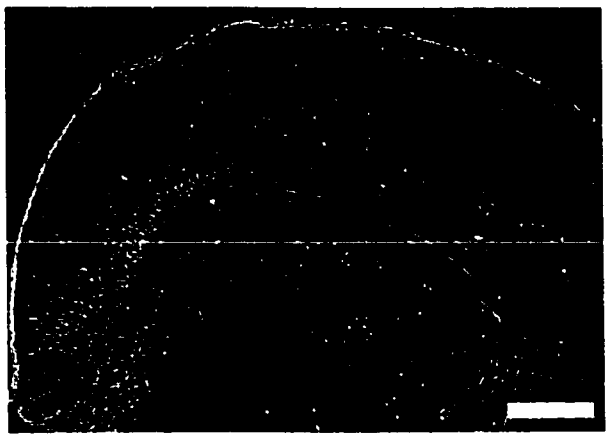

A. +/+

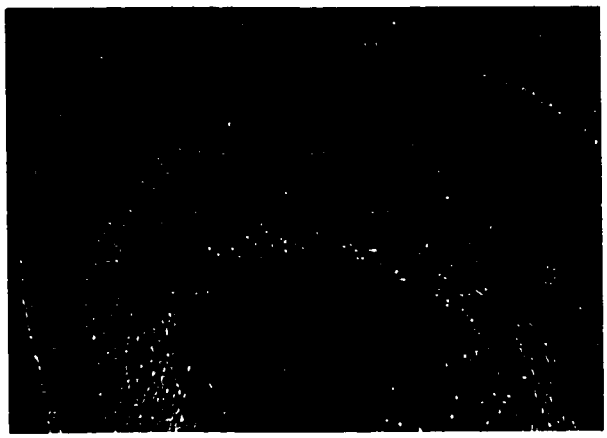

B. +/-

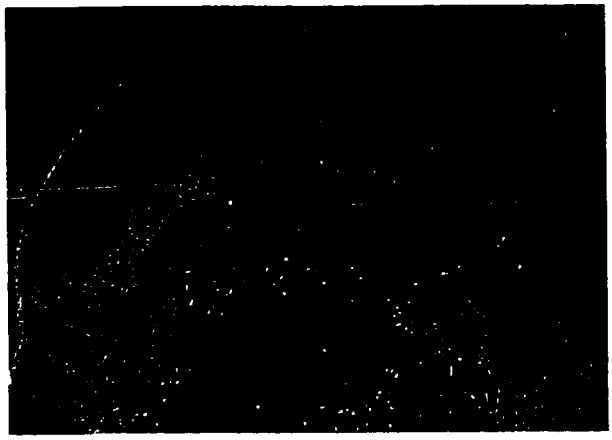

C. -/-

D. +/- Calretinin + DAPI

E. -/- Calretinin + DAPI

specific subcortical brain nuclei. It should be noted that we used a newly developed antibody against calretinin. While the earlier developed antibody recognizes only the calcium bound configuration of calretinin, the antibody we used recognizes the calcium unbound protein as well. The result is far more extensive staining than was observed previously, with increased labeling of corticothalamic axons in the intermediate zone (IZ) and cell bodies in the cortical plate.

Wild type, hemi/heterozygous, and Cx32 null neocortices all show similar patterns of calretinin immunoreactivity (Fig. 3.4): Corticothalamic axons are prominently stained and show the same trajectories through the IZ with terminals at the subplate, possibly reflecting the developmentally transient synapses between thalamus and subplate. A subpopulation of cell bodies in the CP are labeled, with a higher density of labeled cells medially. The highest densities of calretinin labeled cell bodies are in the hippocampal formation, medial to the neocortex.

Cajal-Retzius (CR) cells are the first differentiated neurons in the neocortex (CITE). Reelin, a large glycoprotein secreted by Cajal-Retzius cells, is thought to be the initial signal in a cascade mediating neuronal migration. Therefore, any differences in the number or morphology of Cajal-Retzuis cells might result in deficiencies of neuronal migration. We find no such differences between the three genotypes. A DAPI counterstain with Calretinin labeling (Fig 3.4 D,E) reveals similar morphology, density of CR cells, and the same location within the MZ.

Phosphohistone-3: Phosphohistone-3 (PH-3) is a DNA binding protein found specifically in the chromatin of mitotic cells. As such, its expression pattern provides a snapshot of the location and extent of cell division in a given tissue at a given time. At E17 in the neocortex, generation of neuronal precursors in the Ventricular Zone (VZ) slows considerably. At the same time, there is a surge in the rate of gliogenesis,

Figure 3.5 Phosphohistone 3 immunostaining in E17 Cx32 null neocortex. Pial surfaces are facing up; medial is left. Scale bar=100 uM. Phosphohistone 3 labeling reveals populations of cells undergoing mitosis. Cells are labeled predominantly at the ventricular surface and overlying SVZ, showing comparable numbers and distributions of mitotic cells in +/+, +/-, and -/- neocortex.

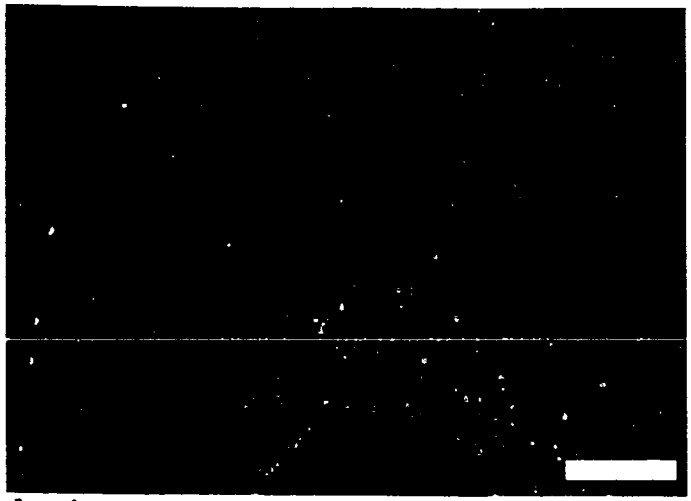

A. +/+

B. +/-

C. -/-

primarily in the SVZ and IZ. These proliferating glial precursors have been referred to as the secondary proliferative population (SPP) (cite Takahashi). The staining pattern we observe for PH-3 effectively mirrors the previously described dynamics of cell generation.

In all three genotypes, a high density of labeled mitotic cells can be seen at the ventricular surface of the neocortex (Fig. 2.6), likely representing the final divisions of neuronal precursors. A larger number of labeled cells are scattered throughout the SVZ, characteristic of glial precursors belonging to the SPP. Although we did not perform counts of labeled mitotic cells, the density and distribution of these cells do not appear to be different in wild-type, hemi/heterozygous, or Cx32 null neocortex.

Voltage-gated sodium channel alpha subunit, brain type II: There is a paucity of previous work describing the developmental expression patterns of specific sodium channel subtypes in the neocortex. This is surprising, considering the importance of specific patterns of sodium channel expression to the functional identity of neurons in the adult brain. We examined the expression of the Brain Type II sodium channel Alpha subunit (Na AlphaII) as a marker for the development of mature excitability properties.

Interestingly, Na Alpha II showed an expression pattern very similar to calretinin, with dense staining in subplate and lower levels of CP and labeling of corticothalamic axons (Fig. 3.6). This pattern was the same for wild type, hemi/heterozygous, and Cx32 null neocortex.. A large subpopulation of cell bodies in the CP were labeled, predominantly in the lower layers. Also worth noting is the labeling of a smaller number of cell bodies in the VZ, SVZ, and IZ

Radial glial cell marker RC2: Radial glial cells provide the infrastructure necessary for neuronal migration. A visualization of their morphology and density in the

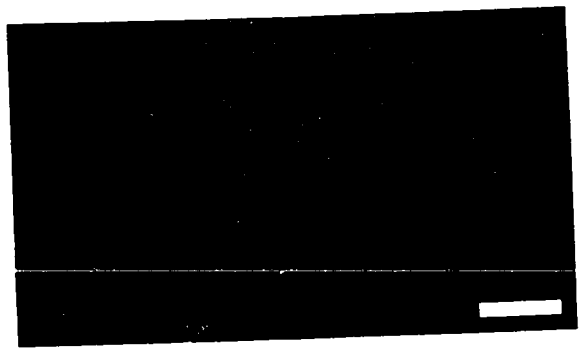

A. +/+

B. +/-

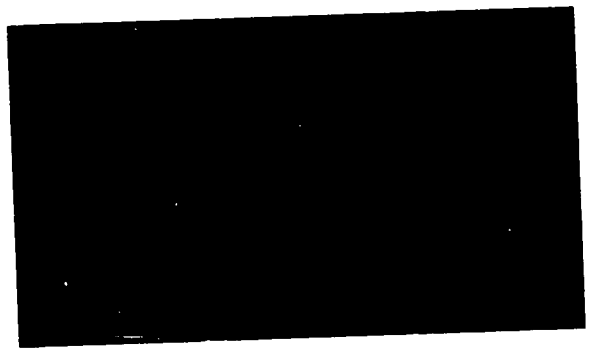

C. -/-

Figure 3.6. Immunostaining for voltage-gated sodium channel alpha subunit, Brain Type II in E17Cx32 null neocortex. Pial surfaces are facing up; medial is left. Scale bar=100 uM. Note dense staining in subplate and lower levels of the CP, a pattern similar to that seen for calretinin. Staining patterns do not appear appreciably different between genotypes.

Cx32 null neocortex might therefore reveal deficiencies in normal neuronal migration patterns. The antibody RC2 has long been used as a specific marker for radial glia and has formed the basis for some of the definitive studies of radial glial morphology and how it changes during development (Hatten et al.).

Results of RC2 immunostaining are shown in Figure 3.7. All three genotypes show normal, classic radial glial morphology. Labeled radial glial cells extend processes that span the cortical wall, with attachments at the ventricular and pial surfaces. The highest density of fibers are seen in the IZ and SVZ, consistent with earlier observations of Gaddiseux et al. at E17 in the mouse (cite). Also prominent is the bundle of radial glial fibers forming the boundary between neocortex and striatum, a boundary that is postulated by some authors to limit neuronal migration between the two structures (Fishell, Stoykova et al.).

C. Evidence for an altered pattern of Cx26 expression in Cx32 null neocortex.

From the results described above, it appears that Cx32 is not necessary for normal neocortical neurogenesis at its culmination at E17. The apparently normal development in the absence of Cx32 could, however, result from a compensatory change in the expression of one or more other connexins. To test this hypothesis, we compared the expression levels of Cx26 in wild type, hemi/heterozygous, and Cx32 null neocortex using the methodology outlined in the previous section for quantifying immunostaining.

Images of Cx26 immunostaining in the three genotypes can be seen in Figure 3.8 processed for image analysis.

When compared quantitatively with wild type and hemi/heterozygous littermates, Cx32 null brains show a striking difference in Cx26 expression pattern (Figure 3.8). The hemi/heterozygous and wild type brains both show a Cx26 staining pattern similar to that

Figure 3.8 Analysis of Cx26 immunoreactivity in E17 Cx32 null neocortex. A., B., and C. are images of +/+, +/-, or -/- necortices immunostained for Cx26 and processed for quantification of immunoreactivity as described in Chapter 2. Pial surfaces are facing up; Bins are 200uM wide. Arrows in C. show the correspondence between bins 1-10 and cytoarchitectonic divisions. Cx32 null neocortex (C.) shows Cx26 immunostaining that is more robust and uniform that that of the wild type, or hemi/heterozygous littermates (A. and B., respectively). The underlying graph shows immunoreactivity (average gray values on a 0 to 255 scale) vs. cortical bin in one +/+ brain, one +/-, and two -/-. Note the striking similarity in patterns between the two -/- brains that is clearly distinct from +/- and +/+ brains.

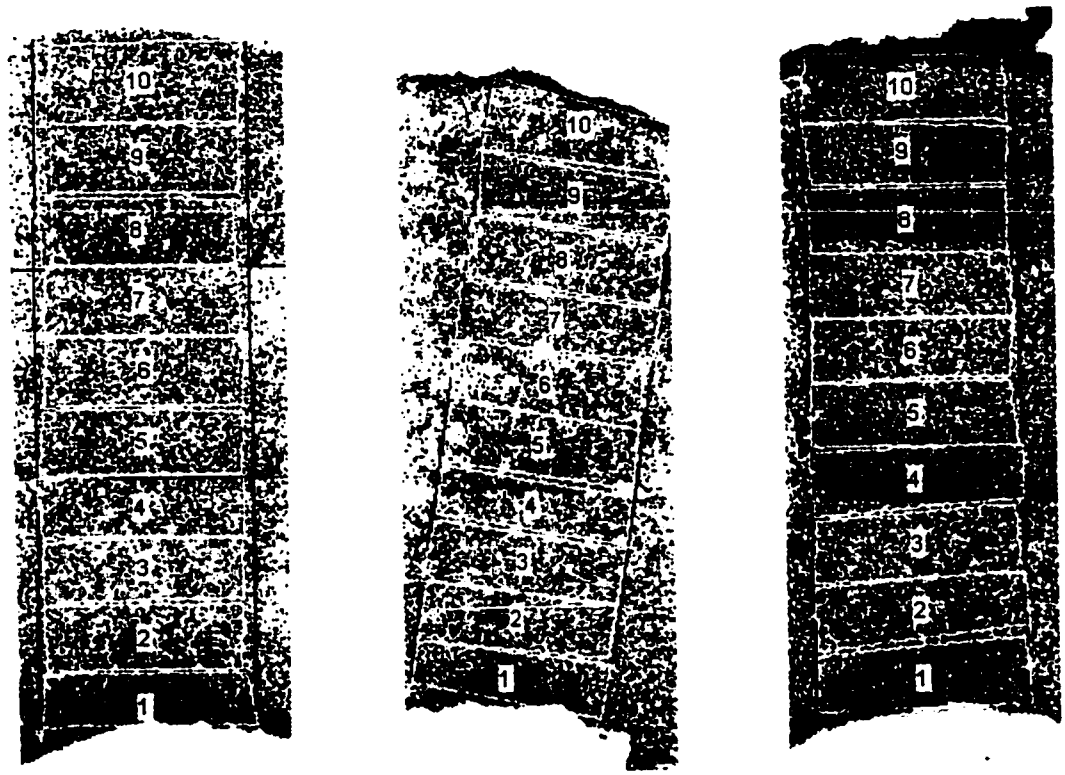
10
9
8
7
6
5
4
3
2
1

A. +/+ B. +/- C. -/-

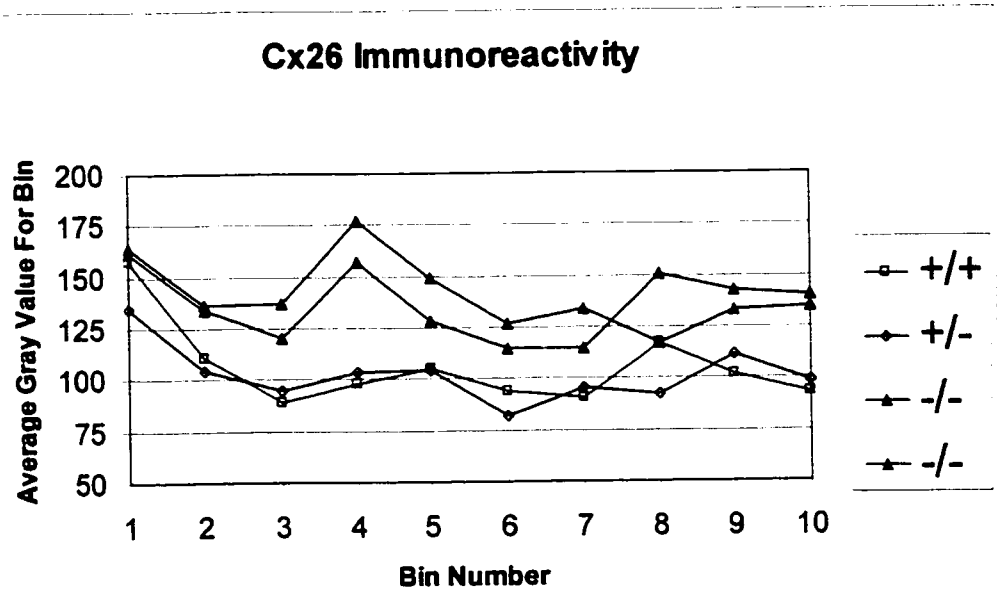
Cx26 Immunoreactivity
Average Gray Value For Bin
200
175
150
125
100
75
50
1
2
3
4
5
6
7
8
9
10
Bin Number
+/+
+/-
-/-
-/-

reported at E17 in the previous section, with markedly reduced staining in IZ and adjacent regions (Bins 4-6). The two Cx32 null brains, in contrast, show patterns of Cx26 staining intensity that are relatively consistent across the cortical wall, without a decrement in staining through the IZ. Also striking is the degree to which the staining patterns of the two Cx32 null brains are in agreement with one another. Since tissue availability was a limiting factor in these studies, we had an insufficient sample from which to draw statistical inferences. Nonetheless, these results provide preliminary evidence for a compensatory change of Cx26 expression in Cx32 null mice.

Results 3

Discovery and characterization of DECORE, a novel developmentally expressed cortex-specific protein.

As mentioned in the first results section, certain lots of polyclonal anti-Cx32 antibody showed an intriguing labeling pattern in later embryonic stages that was found to arise from cross reactivity with another antigen in addition to Cx32. Particularly interesting was the fact that this labeling was intracellular and occurred in a distinct subpopulation of cells exclusively in the cortex (comprising neocortex and hippocampus). Since we observed this pattern in Cx32 null mice, it was apparent hat this antigen was not Cx32. To our knowledge, no antigen with this expression pattern has been described in the literature. We have named the protein recognized by this antibody DECORE for Developmentally Expressed CORtical Epitope. Below we describe the developmental expression pattern of DECORE and an initial characterization of the protein.

A. DECORE is first expressed during late neurogenesis in a subpopulation of postmitotic cells exclusively in the cortex.

DECORE first begins to shows robust expression at E17, the final day of neocortical neurogenesis. This expression pattern is shown in a low power montage (Figure 4.1). From this perspective, it can be seen that a subpopulation of cell bodies are labeled and that these cells are located exclusively in the cortex, from its medial to lateral regions.

The identity of the cells belonging to this subpopulation may be deduced, in part, by their positions within the cortical wall (Figure 4.2). For example, the DECORE

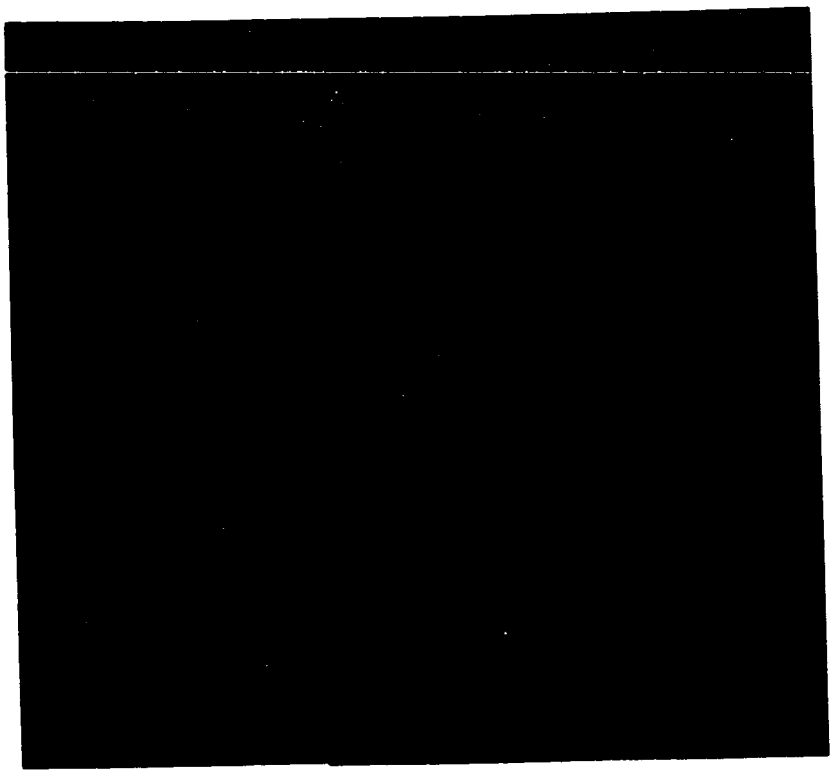

Figure 4.1. DECORE labeling is seen in a subpopulation of cells exclusively in the cortex. Low power montage of DECORE/Cx32 immunolabeling at E17. Dorsal is up. Medial is left. Scale bar=250uM. DECORE expression is defined, and distinguished from Cx32 labeling, by dense intracellular immunoreactivity in a subpopulation of cells exclusively in the cortex. Note absence of DECORE labeled cells in the striatum, ventral to the cortex.

expression pattern is not seen in proliferating cell populations in the VZ/SVZ, which continue to show only membrane immunolabeling for Cx32[2]. From the expression pattern through the other zones, it appears that DECORE labeled cells are predominantly post-mitotic. In the ventricular to pial direction, DECORE expression first occurs among Among some cells in the IZ, the DECORE staining pattern reveals a spindle shaped cell body, with a single process oriented radially toward the pial surface, a morphology characteristic of migrating neurons (Figure 4.2, arrows).

B. At E17, DECORE is expressed in a subpopulation of migrating cells in the IZ.

From the time the IZ is first visible in early to mid neurogenesis, it is composed primarily of migrating neurons *en route* to the CP. Neurons in the neocortex migrate tangential to the ventricular surface or radially, along the processes of radial glia (Pearlman, Faust et al. 1998). We observed that cells in the IZ at E17 with DECORE immunoreactivity often have a morphology suggestive of radially migrating neurons. We therefore sought to clarify the relationship between radial migration and DECORE cytoplasmic immunoreactivity. E17 forebrain sections were triple labeled: double immunolabeled for DECORE and radial glial marker RC2 and counterstained with DAPI. Although DAPI is a fluorescent nuclear stain, the cytoplasm is also outlined by diffuse fluorescence. This labeling paradigm allowed us to visualize the morphology of all cell bodies in the section and their relationships to the labeled radial glial processes. Cells were considered to be radially migrating if they showed both a characteristic spindle shape and proximity to a radial glial process. We could thus ascertain which of these cells showed DECORE immunolabeling.

Figure 4.3 shows a representative triple labeled section of the E17 IZ. Four distinct cell types may be seen: cells with a radially migrating configuration with and without DECORE labeling and cells without a radially migrating configuration with and without DECORE labeling. Therefore, at the developmental time from which the section was taken, cells with DECORE immunolabeling represent a subpopulation of migrating

[2] We reiterate that the anti-Cx32 antibody which produces this labeling pattern that we

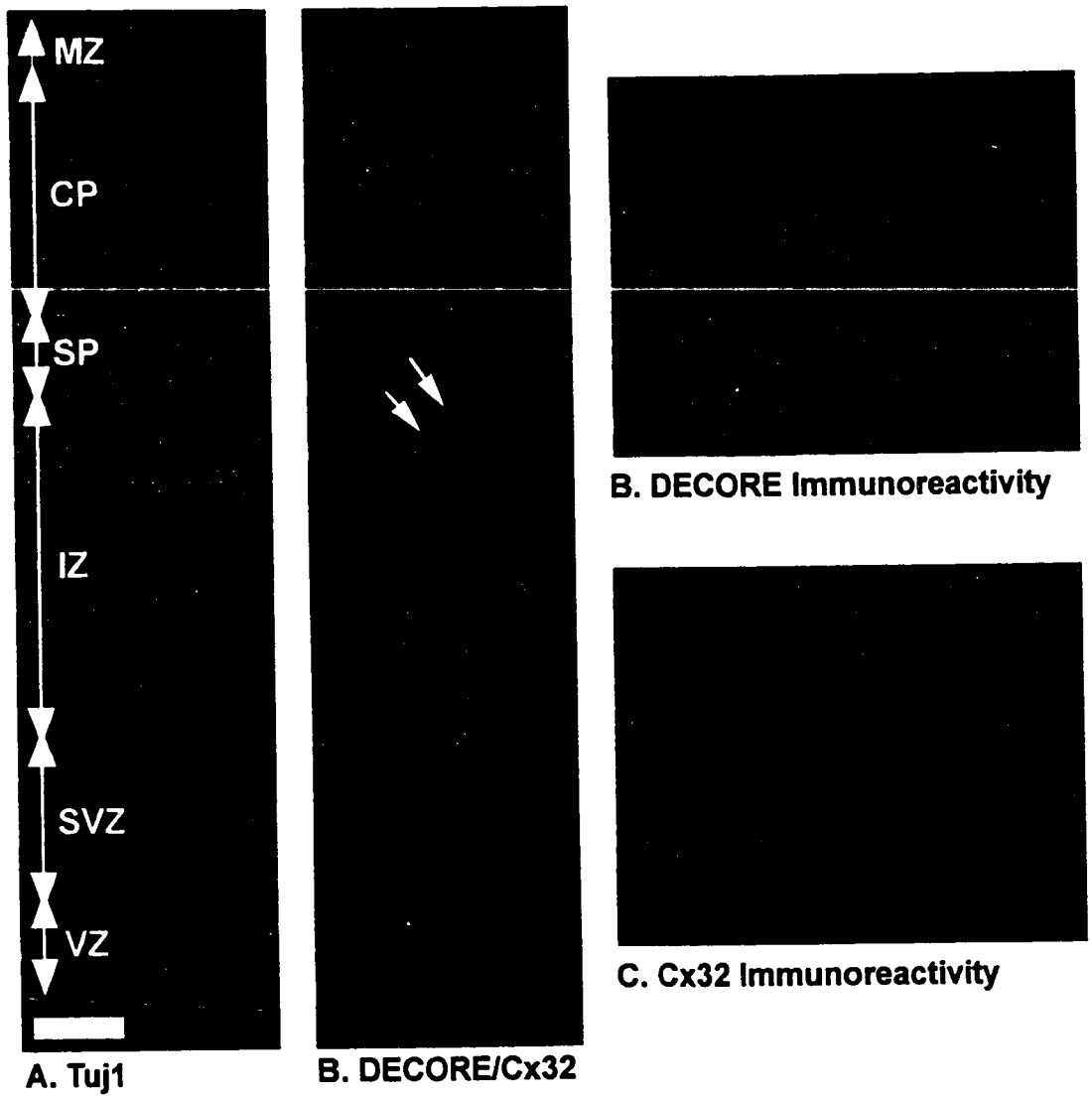

Figure 4.2 DECORE labeling is seen predominantly among postmitotic cells. Adjacent sections of E17 neocortex immunostained for Tuj1 (A.) and DECORE/Cx32 (B.) show the distribution of DECORE labeling in relation to the cytoarchitectonic divisions of the cortical wall. Scale bar=50uM. Note the absence of DECORE labeled cells in the VZ and SVZ, the proliferative populations. DECORE labeling occurs among cells in the mid IZ (with a radially migrating morphology denoted by arrows) and extends through the CP. C and D. distinguish the intracellular DECORE labeling pattern in the outer CP (C.) from the membrane immunoreactivity pattern in the VZ, identical to that seen with other lots of antibodies that recognize Cx32, but do not label DECORE. cells in the outer IZ and SP and is most predominant in the outer CP.

---

designate as DECORE, continues to show membrane immunolabeling for Cx32.

Figure 4.3. DECORE labeled cells represent a subpopulation of migrating neurons in the IZ. E17 Intermediate zone (IZ) triple labeled for DAPI, DECORE/Cx32, and radial glial marker RC-2. DECORE immunolabeling is seen in a subpopulation of migrating cells in the IZ. RC-2 labels processes of radial glia (in red). All nuclei in the section are counterstained with DAPI (blue). Cells with DECORE expression are FITC labeled and therefore appear blue/green against the DAPI counterstain. Radially migrating cortical neurons have a characteristic elongated morphology and are associated with radial glia. Note that both DECORE labeled (red arrow) and DECORE unlabeled (yellow arrow) cells can be seen in this radially migrating configuration. Scale bar = 20 uM. Ventricular surface is down.

cells. More specifically, they comprise a subpopulation of radially migrating cells. It is more difficult to interpret the cells not showing a radially migrating morphology. These cells might be tangentially migrating neurons but they could also be radially migrating neurons sectioned in a plane in which the classic morphology and proximity to radial glia are not apparent.

C. A subpopulation of cells with DECORE immunoreactivity may represent neurons that will form the upper cortical layers II/III.

It is evident that cells with DECORE immunoreactivity represent a subpopulation of cells in the developing neocortex. However, the proportion of cells showing this pattern and their distribution through different neocortical regions are not readily apparent by DECORE immunostaining alone. To address this issue, we analyzed E17 forebrain sections immunostained for DECORE and counterstained with DAPI. Color digital images of the dorsolateral cortical wall were taken serially using FITC (for DECORE staining) and DAPI filters.

Figure 4.4 shows the distribution of DECORE labeled cells across the cortical wall. The VZ and SVZ, the proliferative zones of the E17 neocortex, show only membrane immunoreactivity for Cx32. Cells with the DECORE immunoreactivity pattern first appear in the outer IZ (in the IZ/SP, approximately 30-50% of cells show DECORE staining). The proportion of DECORE immunolabeled cells increases across the CP in the ventricular to pial direction until a maximum of approximately 85% is reached in the outermost fifth of the CP. The birth times and migration patterns of neurons that form the specific neocortical layers have been well established (McConnell 1995; Polleux, Dehay et al. 1997; Takahashi, Goto et al. 1999). The classically described "inside-out" pattern of neocortical development arises from waves of migrating neurons forming consecutively more superficial layers. Based on what is known about the events at E17, the cells in the outer CP, with the highest percentage of DECORE immunoreactivity, form the rudiments of cortical layers II/III. At this stage many of the cells that will form layers II/III are still migrating through the IZ

and lower levels of the CP. It is therefore possible that DECORE immunolabeled cells in these lower levels are also destined for layers II/III, particularly cells in the radially migrating configuration. There is a dramatic decrement of DECORE labeled cells in the MZ, where membrane Cx32 immunoreactivity predominates. The MZ will form layer I in the mature neocortex.

D. The birth order dependence of DECORE expression is evident from its expression in the mouse Disabled 1 *mutant.*

Based on our observation that DECORE labeling first appears late in neurogenesis in a subpopulation of postmitotic cells concentrated in the outer CP, we hypothesized that DECORE expression is characteristic of later born cells. We tested the possible birth-order dependence of DECORE expression by examining neocortices of newborn mice lacking the *Disabled 1 (Dab1)* gene. *Dab1* was the gene found to be deficient in the *Scrambler* mutant, which along with the classically described mutant *Reeler*, shows an altered pattern of neuronal migration, resulting in the formation of effectively inverted cortical layers (cite Howell et. al.). Dab1 is a cytoplasmic adaptor protein that, in conjunction with low density lipoprotein receptors VLDLR and ApoER2, controls neuronal migration by modulating responses to Reelin secreted by Cajal-Retzius cells in the MZ (Howell et al.).

We predicted that, if DECORE expression is characteristic of cells generated later in neurogenesis, then the distribution of DECORE labeled cells should be inverted in *Dab1* null mice. Alternatively, if DECORE labeled cells show the same distribution in *Dab1*null neocortex as they do in heterozygous or wild-type, then DECORE expression is likely mediated in a manner independent of cell birth order.

Results of DECORE immunostaining in *Dab1* null and heterozygous neocortex are shown in Figure 4.5. In *Dab1* null neocortex, DECORE labeled cells are concentrated more in the lower CP and thus their distribution appears inverted compared to the heterozygote. Interestingly, there also appear to be larger overall numbers of DECORE labeled cells in the *Dab1* null neocortex. This obvious disruption in the *Dab1*

Figure 4.4. Spatial distribution of cells showing DECORE immunostaining at E17. Assembled composite images of E17 neocortical sections immunostained for DECORE/Cx32 (left) and the same section counterstained with DAPI (right). The arrows correspond to the approximate location of the cortical regions. VZ=ventricular zone, SVZ=subventricular zone, IZ=intermediate zone, SP=sub-plate, CP=cortical plate, and MZ=marginal zone. The vertical white lines divide the CP into six bins through the CP in the dorsoventral dimension. Note that the largest proportion of DECORE labeled cells are found in the outermost sixth of the CP, corresponding to what will become layers II/III in the adult neocortex.

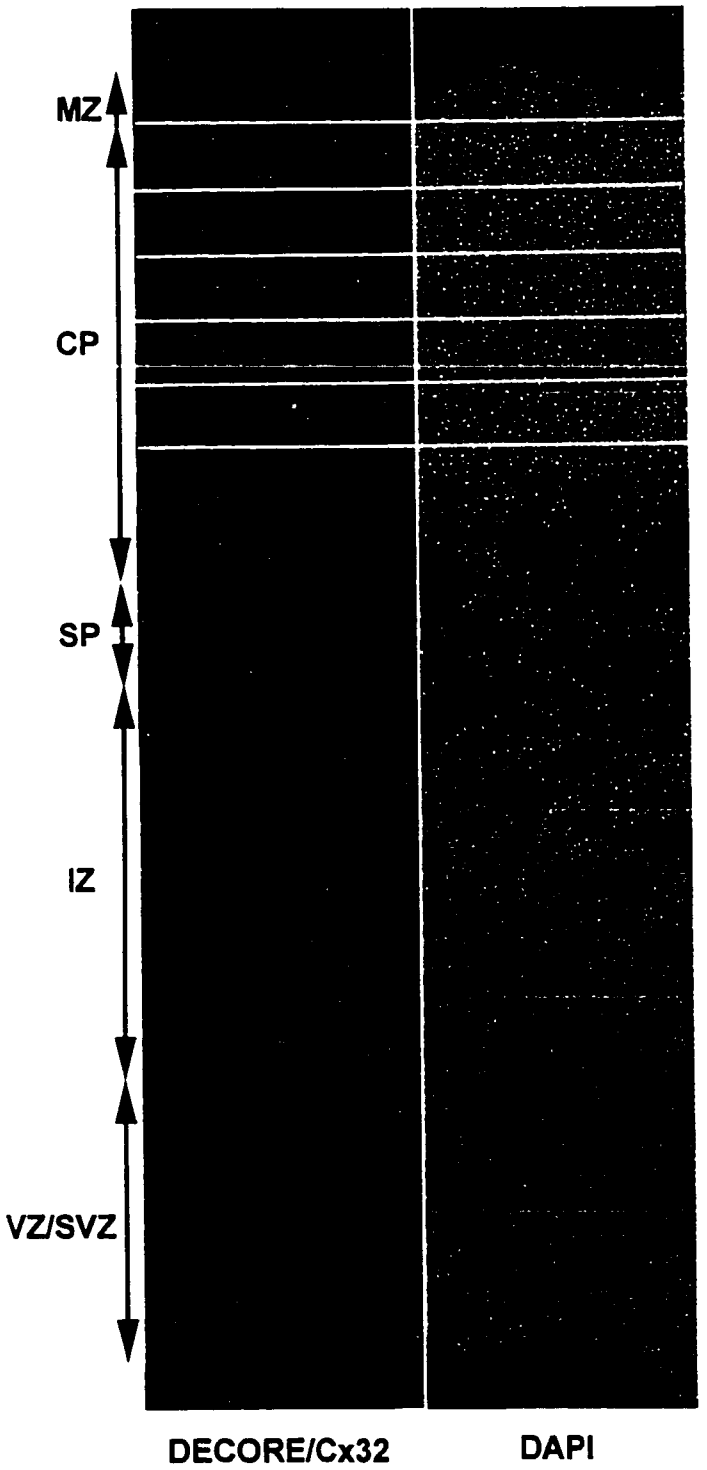

Figure 4.5. DECORE immunoreactivity in the *dab* null neocortex. DECORE immunostaining in sagittal sections of *dab* heterozygote (A.) and homozygous null (B.) neocortex. Scale bar=100uM. Dorsal is up. Rostral is to the right. Note that DECORE labeled cells, predominantly found in the outer CP in dab +/- (and wild-type), are most

labeled cells, predominantly found in the outer CP in dab +/- (and wild-type), are most concentrated in the lower CP of dab -/- mutants. This effective inversion of the DECORE expression pattern strongly suggests that DECORE is developmentally regulated in a manner dependent on cell birth order.
mutant of the normal position of DECORE labeled cells argues strongly for a birth-order dependence of DECORE expression.

E. By P12, DECORE expression shows a distribution across the cortical wall similar to E17, but with proportionally fewer labeled cells.

Immunolabeling of P12 neocortex with the antibody that recognizes DECORE reveals groups of cells with intracellular labeling distributed mostly through the inner and outer neocortical layers (Figure 4.6). Compared to E17, there are proportionally fewer cells showing this pattern. No DECORE labeling is seen in the hippocampus or in the white matter (with few cell bodies).

At higher magnification (Figure 4.7), DAPI counterstaining confirms that the highest density of labeled cells is in the outer cortical layers (Figure 4.7; compare B with DAPI counterstain of the same section in A), with the next highest in the inner layers. The presence of DECORE labeled cells in the inner layers at this stage raises several possibilities (see Discussion). Among the possible interpretations is that DECORE expression might be transient in some cell populations.

At this stage, there is a subpopulation of cells clearly showing perinuclear cytoplasmic labeling (see detail in Figure 4.7D, yellow arrow) standing in contrast to the labeling we designate as DECORE, which appears to be primarily nuclear (Figure 4.7, white arrow). We performed immunostaining in sections of the same brain using the anti-Cx32 antibody that does not cross react with DECORE. The immunostained section in Figure 4.7E shows the same cytoplasmic labeling in a similarly distributed subpopulation of cells, predominantly in the middle cortical layers. It is therefore our contention that this cytoplasmic labeling represents Cx32 and not DECORE.

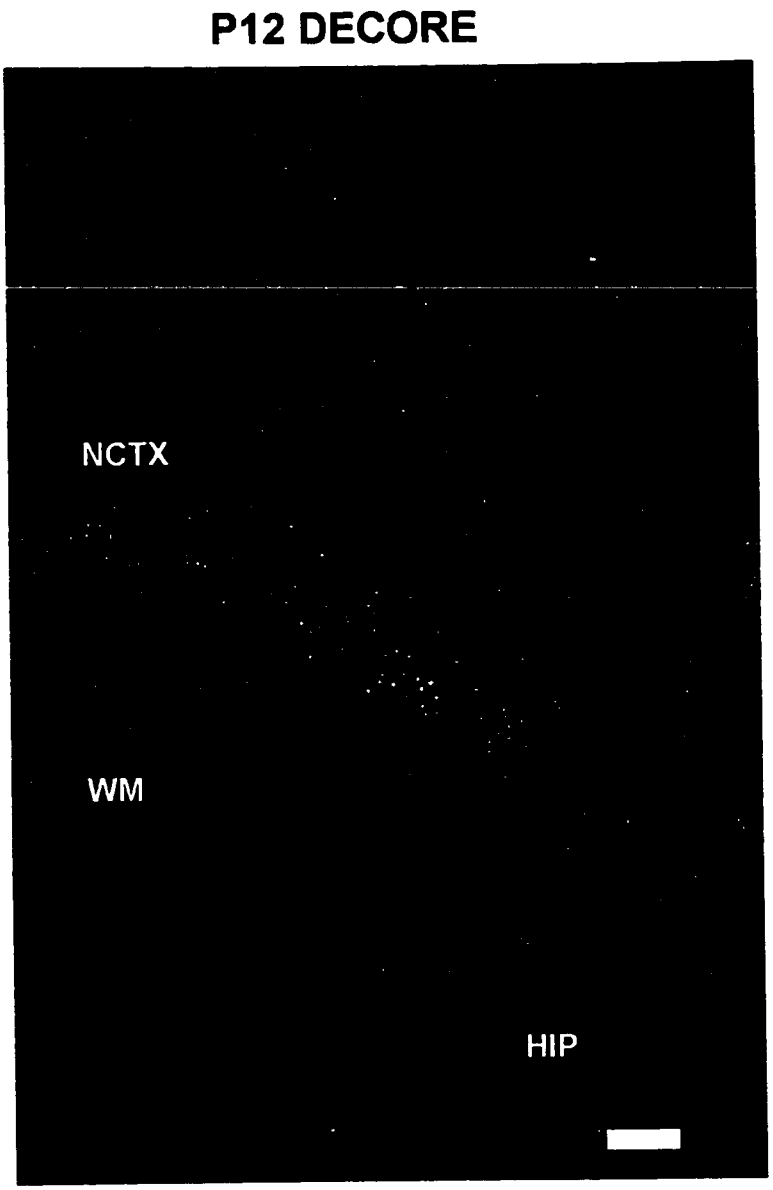

Figure 4.6. DECORE labeling at P12. Scale bar=250um. NCTX=neocortex, HIP=hippocampus, WM=white matter. Dorsal is up. Medial is right. Note that DECORE labeled cells (arrows) are proportionally fewer in number compared to E17 and are concentrated in the outer layers and the deep layers.

Figure 4.7 DECORE distribution across the cortical wall at P12. Immunolabeling with the antibody that recognizes DECORE (B., C., D.) compared to that of the antibody that recognizes only Cx32 (E., F., G.) A. is the same section as B., counterstained with DAPI to show cell density across cortical wall. Scale bar in A=100uM and also applies to B. and E. Scale bar in D. =50uM and also applies to C., F., and G. Dorsal is up. Note highest concentration of DECORE labeled cells in deeper layers and toward the pial surface (detail in C.) With DECORE stained sections, the middle neocortical layers (detail in D.) contain cells with cytoplasmic labeling (yellow arrow, cell with unstained nucleus) as well as the more obvious DECORE intracellular pattern (white arrow), which by contrast appears nuclear. In the equivalent region of the Cx32 immunostained section, only the cytoplasmic staining is apparent (G., yellow arrow).


A. DAPI
B. DECORE
C.
D.
E. Cx32
F.
G.

F. Selective immunoblot analyses identify DECORE as a protein of approximately 110kD.

We sought to isolate the DECORE protein using immunoblot analyses and subsequent immunoprecipitations. Our initial strategy was based on the observation that only certain lots of polyclonal anti-Cx32 antibody cross-reacted with DECORE. However, when these different lots of anti-Cx32 were used to probe blots of membrane protein preparations from P2 forebrain, they failed to show differences with respect to the bands they labeled (data not shown). This observation, coupled with the intracellular immunostaining that defines the DECORE expression pattern, suggested that the DECORE protein is not membrane associated. Accordingly, we performed all subsequent analyses on proteins derived from whole-cell extracts under non-denaturing conditions. Immunoblots performed on these preparations revealed several bands labeled exclusively by the lots of antibody that recognize DECORE (Figure 4.8)

The next challenge was to determine which of these bands might represent the DECORE protein. To address this question, we took advantage of our observation that DECORE expression is exclusive to the cortex (predominantly in the neocortex) and is thus largely confined to the dorsal forebrain. Therefore, by comparing immunoblots of protein extracts taken from dorsal forebrain vs. those from ventral forebrain (containing subcortical structures such as thalamus and striatum), we could determine if any of the bands we observed are unique to the dorsal forebrain. Using this strategy (also summarized in Figure 4.8), we found a band of approximately 110 kD that is unique to dorsal forebrain--our current candidate for the DECORE protein.

We have subsequently performed immunoprecipitations on these dorsal and ventral protein preparations (as outlined in Methods) and have succeeded in isolating the same band unique to dorsal forebrain. Further analyses, using Tandem Mass Spectroscopy are pending for the isolated DECORE candidate protein.

Figure 4.8 Strategy for isolation of DECORE protein and results. A 110 kD candidate protein for DECORE was isolated based on the strategy outlined. Blots of dorsal and ventral (D and V) forebrain derived proteins, when probed with the antibody that recognizes Cx32 (but not DECORE), both show single bands corresponding to the 3-mer of Cx32. In contrast, the antibody that recognizes DECORE labels several bands at higher molecular weights in both D and V samples. Since DECORE is exclusively in cortex (and therefore enriched in dorsal forebrain), the band at approximately 110kD from the D sample is the strongest candidate for DECORE.

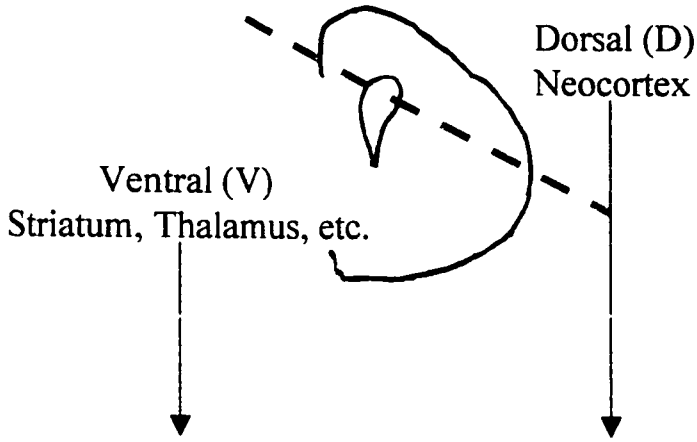

Perform non-denaturing whole cell protein extractions.

Separate proteins by PAGE and blot to membranes.

Probe with Lot 1 antibody (DECORE)

Probe with Lot 2 antibody (Cx32)

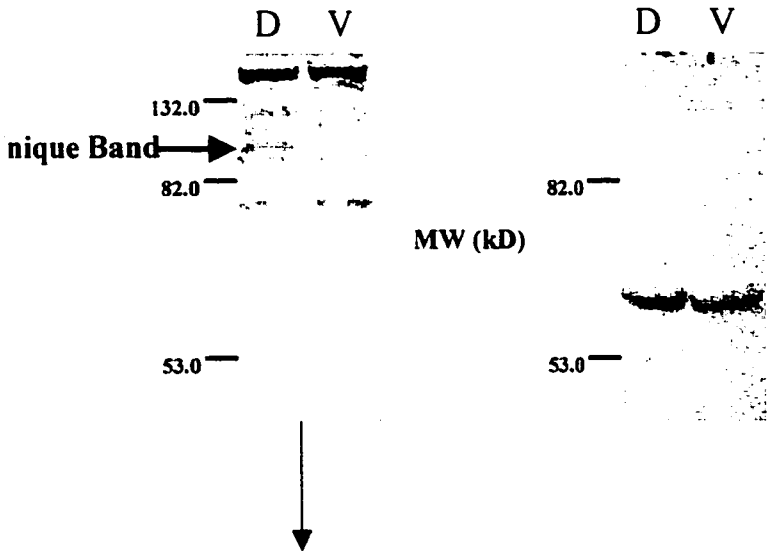

Isolate band by immunoprecipitation and Identify by Tandem Mass Spectrometry.

Chapter 5
Discussion and Conclusions

A. Expression of Cx26 and Cx32 during neocortical neurogenesis

We surveyed the expression of Cx26 and Cx32 in the developing neocortex at embryonic stages representing early, middle, and late neocortical neurogenesis. The purpose of this study was to gain insights into the possible roles for these connexins in mediating the developmental events involved in constructing the neocortex.

In the initial portion of this study, we examined the expression of Cx26 and Cx32 in conjunction with established markers (Tuj1 and BrdU labeling) to visualize concurrent developmental events. From these largely qualitative analyses, we observed that Cx26 and Cx32 are both expressed throughout the cortical wall at all stages of neurogenesis. Although there were some notable differences in temporal and spatial expression patterns for Cx26 and Cx32, it is an important observation that both connexins were represented among proliferating, migrating , and differentiating cells (in the VZ/SVZ, IZ, and CP, respectively). Furthermore, both proliferative cells within the VZ or SVZ undergoing S-phase (BrdU labeled) and those in other stages of the cell cycle displayed Cx26 and Cx32 immunolabeling.

Previous studies have shown that different populations of cells demonstrate dramatic differences in dye coupling patterns, both in terms of cluster size and morphology. For example, dye coupling among migrating neurons within the IZ is significantly reduced compared to proliferative cells in the VZ (Lo Turco and Kriegstein 1991), suggesting a functional decoupling during migration. Within the VZ, mitotic cells at the ventricular surface are excluded from dye-coupled clusters (Bittman, Owens et al. 1997). The fact that these differences in coupling occur despite continued expression of Cx26 and Cx32 suggests that properties of gap junctional coupling in the embryonic neocortex are modulated in ways other than (or in addition to) the differential expression of connexin isoforms.

For the second portion of our study, we asked whether proliferating, migrating, and differentiating cells showed significant differences in Cx26 or Cx32 expression levels *vis-a-vis* immunostaining intensity. In the paradigm described in Chapters 1 and 2, we measured immunolabeling intensity across the cortical wall in 10 evenly sized bins, then regrouped the data from those bins into proliferating (Pro), migrating (Mig), and differentiating (Dif) populations based on their correspondence to the VZ/SVZ, IZ, and CP/SP/MZ, respectively. We performed a one-way analysis of variance (ANOVA) for each connexin at each age, comparing Pro, Dif, and Mig groups (when present at later stages). The threshold of significance was set at $P < .05$. By these analyses, Cx26 showed a significant variation across the cortical wall at E12, E14, and E17. Cx32 showed significant variation only at E12 and E17. Neither connexin showed a significant pattern at E16.

When the patterns were significant at E12 and E14, it was due to the relatively high immunostaining intensity in the outer CP and MZ (bins 9 and 10). It is somewhat paradoxical that post-mitotic cells at E12 and E14 show a higher level of connexin expression, particularly when gap junctional coupling has been shown to be important for normal proliferation of neuronal precursors in the VZ *(LoTurco and Kriegstein 1995)*. It is possible that increased connexin expression underlies the change in coupling configuration among neurons in the preplate and later cortical plate. Alternatively, the increased intensity of immunostaining might reflect a redistribution of connexins rather than increased expression.

The greatest change in the expression patterns of Cx26 and Cx32 seem to occur at E17, when immunostaining intensity for Cx26 drops precipitously in the IZ and SP/inner CP. Although both Cx26 and Cx32 showed statistically significant variation across the cortical wall at E17, the variation is much more dramatic for Cx26. This pattern could reflect a lower cell density in this region (at earlier stages, cell density is relatively homogeneous across the cortical wall), however it is interesting that Cx32 does not show the same relative change. This regional decrease in Cx26 corroborates the previously observed down-regulation of Cx26 in the early post-natal rat neocortex (Nadarajah et al.).

Furthermore, a decrease in Cx26 expression in the IZ may underlie the reduced dye coupling seen among migrating neurons.

Another goal of this second study was to examine how expression patterns of Cx26 and Cx32 varied with respect to one another. By doing so, we could assess the degree to which overlapping expression of Cx26 and Cx32 might be consistent with the formation of heteromeric channels. To perform such a comparison required that we take into account any variations in immunostaining intensity that may be unrelated to relative expression levels of Cx26 and Cx32. Accordingly, we normalized the gray values for each section by setting the bin with maximum immunostaining to one and expressing the values of all other bins in that section as a fraction thereof. As such, we compared relative patterns of Cx26 and Cx32 expression for each stage. We grouped the data to reflect Pro, Mig, and Dif populations as we did in the analyses described.

By our rationale, if normalized patterns are the same (or vary insignificantly) between Cx26 and Cx32, this argues for a stoichiometric representation of each connexin consistent with the formation of heteromeric channels. To test this possibility, we performed two-tailed t tests in Pro, Mig, and Dif groups at each age to compare the variation of Cx26 vs. Cx32. In effect, we were testing a counter-null hypothesis that Cx26 and Cx32 expression patterns are significantly different. Dif cells at E12 and Mig and Dif cells at E16 did not show significant differences (at the $P<.05$ level) in normalized Cx26 vs. Cx32 expression patterns, suggesting even representation of the two connexins. Interestingly, E16 was also the only stage in which neither Cx26 nor Cx32, when analyzed individually, showed significant variation across the cortical wall.

Other cell populations at E12, E14, E16, and E17 did show significant differences in normalized expression patterns of Cx26 and Cx32. These results, however, should not be interpreted in the strictest sense that heteromeric channels do not exist in these cell populations. Rather, these analyses reveal where heteromeric channels are most likely to be found. They do not rule out the presence of heteromeric channels in the other cell populations with overlapping expression of Cx26 and Cx32.

Aside from testing the possibilty of heteromeric channels, these analyses verified the observation that Cx26 is down-regulated relative to Cx32 among Mig populations at E17. As shown in Figure 2-10, the difference between normalized expression levels of Cx26 and Cx32 is significant to a very high level (P=**). An interesting ramification of this data is that Cx32 is most highly represented among migrating cells at E17.

In summary, our analyses of Cx26 and Cx32 expression in the embryonic neocortex indicate that both connexins are expressed throughout neurogenesis, among dividing, migrating, and differentiating cells. Our quantitative analyses show that at most stages, expression levels of Cx26 or Cx32 are significantly different between these cell populations. The most notable exception is E16, when Cx26 and Cx32 both show staining that is uniform across the cortical wall. A dramatic change occurs at E17 in which Cx26 expression is significantly lower among migrating cells. Our comparisons between normalized staining patterns for Cx26 and Cx32 suggest that, of all the stages we examined, heteromeric channels are most likely to form at E12 (among Dif cells) or E16 (all populations).

Further studies will be needed to ascertain the biological significance of these differences. The primary limitation of comparing connexin expression at a gross level between cell populations is its sensitivity. Subtle, but developmentally relevant differences might not be detected by our methods. Furthermore, as our own data attest, connexin expression levels do not always correlate directly with the nature or extent of gap junctional coupling. Gap junctional communication during development more likely involves a dynamic interplay between connexin expression, trafficking, assembly into gap junctions, modulation of gap junction channels, and their degradation. Nonetheless, our survey of Cx26 and Cx32 expression during neocortical neurogenesis provides initial results compelling enough to warrant future investigation.

B. Neocortical Development in the Cx32 Null Mouse

Our observation that Cx26 and Cx32 are abundantly expressed in the embryonic neocortex at critical times in development suggested that these two connexins may be

involved in mediating developmentally important cell-cell interactions. The most direct method of testing this possibility experimentally is to examine neocortical development in the absence of Cx26 and/or Cx32. To a certain extent, nature has already performed this experiment on humans. Mutations in Cx26 result in certain forms of sensorimotor deafness and mutations in Cx32 are responsible for X-linked Charcot-Marie-Tooth disease, an inherited peripheral nervous disorder (citations). Yet for obvious reasons, embryonic neocortical development has not been studied in individuals carrying these mutations.

Mouse knockout lines for Cx26 and Cx32 have been constructed (Willecke et.al). The Cx26 null phenotype is embryonic lethal at E10 (2 days prior to the start of neocortical neurogenesis) as a result of deficiencies in placental glucose uptake. Cx32 null mice are by contrast, viable and fertile. Their most obvious deficiencies are in liver function, a likely result given the abundant presence of Cx32 in the liver. Older adult mice (> 6 months) develop peripheral nerve deficiencies reminiscent of CMTX, although it is not a precise phenocopy of the human disease (See Willecke et.al. 1999 for review).

We examined the neocortices of Cx32 null mice for evidence of developmental abnormalities. Our study represents the first investigation of a developmental role for Cx32. As mentioned above, we chose to analyze E17 because it represents the culmination of neocortical neurogenesis. Furthermore, E17 was the stage in which we observed the largest changes in E17 expression, particularly in relation to Cx26. We used a panel of immunological markers to assess specific developmental parameters in the Cx32 null neocortex, namely cell proliferation, migration, and neuronal differentiation. We obtained for analysis one E17 litter containing two Cx32 null embryos. Because of the limited statistical power of our sample size, the results we report are largely qualitative descriptions.

Three of the markers we used (Tuj1, fluorescent Nissl stain, and Hematoxylin/Eosin stain) allowed us to visualize the VZ and make size comparisons between Cx32 null, hemi/heterozygous, and wild-type brains. The size of the neocortical VZ is a correlate of proliferative activity of neuronal precursors (Caviness). The

rudimentary presence of the VZ at E17 therefore reflects the normal slowdown in division toward the end of neurogenesis. We found no substantive differences in VZ size between the three genotypes. If dynamics of division of neuronal precursors are maintained, then equal sizes of VZ indicate a roughly equal neuronal output. Immunostaining for Phophohistone 3 provided a direct visualization of mitotic cells. Again, we observed no real differences in density or locations of mitotic figures.

We used the marker RC-2 to look for changes in radial glial morphology that might indicate a deficiency in neuronal migration. In the Cx32 null neocortex, we saw no differences in morphology of radial glia or the trajectories of their processes. Furthermore, Tuj1, Fluorescent Nissl, and H&E stains all indicated a normal size and density of cells in the CP, evidence that the endpoint of neuronal migration was unaffected. Along with Tuj1, antibodies to Calretinin and the sodium channel alpha II subunit served as markers of neuronal differentiation. However, unlike Tuj1, these two markers labeled specific subpopulations of differentiated neurons. Cx32 null neocortex showed a patterns of immunoreactivity for calretinin and the alpha II subunit that were similar to that of its hemi/heterozygous and wild-type littermates, both in terms of cell populations labeled and (when visible) their axonal projections.

The apparently normal development of the Cx32 null neocortex suggested that either 1. Development is able to proceed normally with reduced gap junctional coupling in the absence of Cx32 or 2. An up-regulation of another, functionally similar connexin compensates for the loss of Cx32. We chose to test the latter hypothesis and to start by comparing Cx26 expression in normal and Cx32 null neocortex. We performed the same image analyses described in chapter 2 to quantify the intensity and distribution of immunostaining across the cortical wall. In both of the Cx32 null neocortices we examined, we found a strikingly similar pattern of increased Cx26 expression, particularly in the IZ.

These results are preliminary and based on a small sample size. Nonetheless, it is interesting to note that the expression pattern of Cx26 in Cx32 null neocortex closely resembles the pattern of Cx32 we observed for wild-type neocortex in Chapter 2. In

effect, it appears that the absence of Cx32 prompts a compensatory up-regulation of Cx26. However, to call this an up-regulation may be misleading. Our observations may instead reflect a suppression of the down-regulation we observed for Cx26 at E17, especially in the IZ. If this pattern is verified by further studies, then it may explain, in part, how necortical development could proceed normally in the absence of Cx32. It would furthermore attest to the importance of gap junctional communication to neocortical development.

While we were collecting data from the Cx32 null embryos, a paper came to press describing a CNS phenotype in the adult Cx32 null mouse. Sutor et al. performed intracellular recordings in cells of neocortical layers II/III from slice preparations of Cx32 null adult mouse forebrain (Citation). They found that approximately half of the layer II/III neurons showed what they termed hyperexcitability—a tendency to respond to afferent stimulation with delayed and large glutamatergic excitatory post synaptic potentials. The authors attributed this hyperexcitability in part to increased input resistance, but also to deficiencies they observed in axonal myelin sheaths. Otherwise, their histological data corroborated our evidence that Cx32 null neocortex shows no gross anatomical differences.

It would be worthwhile to perform similar electrophysiological analyses, perhaps by patch clamp, to compare the ionic currents and resulting excitability profiles in neurons of normal and Cx32 null neocortex at E17. This set of experiments could ascertain whether the hyperexcitability the authors observed in neurons in the adult neocortex is indeed due to altered myelination or if the absence of Cx32 results in developmental changes in intrinsic membrane properties. Since myelination of cortical neurons occurs mostly during postnatal development (cite), any differences in excitability at E17 could be attributed to the neuron itself or to its pattern of gap junctional coupling.

C. Discovery and Characterization of DECORE

We discovered the DECORE protein somewhat serendipitously, as a cross-reacting target of particular lots of commercially manufactured polyclonal anti-Cx32

antibodies. Rather than dismiss this cross-reactivity as artifact, we chose to learn more about the target of this antibody because of its unique expression pattern, specific to a subpopulation of cells exclusively in the cortex. Closer examination yielded these observations about the antigen : It first begins to show robust expression at E17, the final day of neurogenesis. The label is intracellular, allowing us to differentiate this antigen from Cx32, which shows only membrane immunoreactivity at E17. Labeled cells are very distinct from unlabeled cells and they are post-mitotic, judging by their exclusion from the VZ/SVZ. A number of labeled cells are found in the IZ as a subpopulation of migrating neurons. Finally, these cells are most highly concentrated in the outer CP. Subsequent to these observations, we assigned this antigen the name DECORE for reasons mentioned in Chapter 4.

The timing of DECORE expression and the distribution of labeled cells in the IZ and CP led us to speculate that DECORE is developmentally regulated in a manner dependent upon when a cell is born during the sequence of neocortical histogenesis. By the famous inside-out scheme of neocortical development advanced by Angevine and Sidman (Angevine and Sidman 1961), later born neurons form the outer cortical layers II/III. We therefore hypothesized that DECORE is a marker for cells that will eventually form layers II/III. Historical precedent dictated that we use Thymidine or BrdU birthdating studies to test this hypothesis. However, our initial attempts at the latter produced ambiguous results stemming from difficulties with cells maintaining their label after the necessary long post BrdU survival times.

So by necessity, we found another (arguably more elegant) way to test our assertion. We examined the distribution of DECORE labeled cells in mouse knockouts of the *Disabled (dab)* gene. As described previously, absence of Dab resulted in a phenotype identical to the *Reeler* mouse, with a reversal in the order of neuronal migration and neocortical layer formation. We predicted that if DECORE labeled cells represented later born neurons, then these cells would be situated in the lower, rather than upper, layers in the *dab* null mouse. As Figure 4-5 demonstrates, this prediction was

borne out in striking clarity. DECORE labeled cells are indeed concentrated predominantly in the lower layers.

Up to this point, we had been looking at DECORE expression in late embryonic and early postnatal neocortex. When older postnatal neocortical tissue became available at P12, we examined DECORE expression to address whether expression persists to this stage and if so, whether DECORE expressing cells are situated in layers II/III like we predicted. Our results were mixed. Although DECORE is expressed at P12 and the subpopulation of cells are most concentrated in layers II/III, the proportion of cells expressing DECORE is much smaller than at earlier stages (See Figure 4-6). Moreover, DECORE expression is seen in a large number of cells in lower layers V and VI. The smaller relative numbers of DECORE expressing cells at E12 compared to E17 may possibly be attributed to the proliferation of glial cells during postnatal development. Therefore, the number of DECORE expressing cells may stay constant through postnatal development, but become effectively diluted by other cell types.

However, the presence of DECORE labeled cells in lower layers at P12 might provide evidence to the contrary, suggesting that DECORE expression is transient in different cell types. This possibility counters our notion that DECORE expression during late embryogenesis and early postnatal development is characteristic of cells that will form layers II/III. Furthermore, this result is somewhat paradoxical in light of our observations of DECORE expression in *dab* null mice which provide strong evidence for a birth order dependent pattern. This discrepancy might be resolved by the explanation that cells in the lower CP at E17 are not migrating neurons bound for layers II/III, but are in fact resident neurons that begin to express DECORE at E17. In contrast, migrating cells in the IZ may be bound for layers II/III. Therefore, DECORE might show a bipartite expression pattern.

Although DECORE shows an expression pattern suggestive of a developmental role in the neocortex, we have no direct evidence for a specific role. The most obvious distinguishing characteristic of DECORE is that it is expressed exclusively in the cortex. According to the prosomeric model of brain development advanced by Rubenstein et

al.(cite), the developing forebrain, or prosencephalon, is organized into domains characterized by unique patterns of gene expression, much like rhombomeres in the hindbrain. Although an attractive model, the idea of a prosomeric organization is thus far limited by a paucity of genes showing expression domains consistent with the anatomical demarcations of forebrain structures. It is possible that DECORE may represent a prosomeric gene that confers a region specific identity to cortical structures, possibly within layers. It is an interesting coincidence that the layers where DECORE predominates (layers II/II and V) are the layers with the highest density of commisural or subcortical projection neurons (cite). The DECORE expression pattern we observed at P12 appeared to be localized to nuclei, especially when compared to the cytoplasmic localization of Cx32. It is therefore tempting to speculate that DECORE may be a transcription factor involved in cell specification. At this point, all we can ascertain about the molecular structure of DECORE is its approximate molecular weight of 110 kDa. We will anxiously await the results of further analyses of this protein.

References

Anzini, P., D. H. Neuberg, et al. (1997) Structural abnormalities and deficient maintenance of peripheral nerve myelin in mice lacking the gap junction protein connexin 32. J Neurosci 17(12): 4545-51.

Barami, K., B. Kirschenbaum, et al. (1994) N-cadherin and Ng-CAM/8D9 are involved serially in the migration of newly generated neurons into the adult songbird brain. Neuron 13(3): 567-82.

Barker, J. L., T. Behar, et al. (1998) GABAergic cells and signals in CNS development. Perspect Dev Neurobiol 5(2-3): 305-22.

Barrio, L. C., T. Suchyna, et al. (1991) Gap junctions formed by connexins 26 and 32 alone and in combination are differently affected by applied voltage. Proc Natl Acad Sci U S A 88(19): 8410-4.

Behar, T. N., A. E. Schaffner, et al. (1998) Differential response of cortical plate and ventricular zone cells to GABA as a migration stimulus. J Neurosci 18(16): 6378-87.

Behar, T. N., C. A. Scott, et al. (1999) Glutamate acting at NMDA receptors stimulates embryonic cortical neuronal migration. J Neurosci 19(11): 4449-61.

Bevans, C. G., M. Kordel, et al. (1998) Isoform composition of connexin channels determines selectivity among second messengers and uncharged molecules. J Biol Chem 273(5): 2808-16.

Bittman, K., D. F. Owens, et al. (1997) Cell coupling and uncoupling in the ventricular zone of developing neocortex. J Neurosci 17(18): 7037-44.

The Boulder Committee. (1970) Embryonic vertebrate central nervous system: revised terminology. The Boulder Committee. Anat Rec 166(2): 257-61.

Bruzzone, R. and C. Ressot (1997) Connexins, gap junctions and cell-cell signalling in the nervous system. Eur J Neurosci 9(1): 1-6.

Bruzzone, R., T. W. White, et al. (1996) The cellular Internet: on-line with connexins. Bioessays 18(9): 709-18.

Bukauskas, F. F., C. Elfgang, et al. (1995) Heterotypic gap junction channels (connexin26-connexin32) violate the paradigm of unitary conductance. Pflugers Arch 429(6): 870-2.

Caviness, V. S., Jr., T. Takahashi, et al. (1995) Numbers, time and neocortical neuronogenesis: a general developmental and evolutionary model. Trends Neurosci 18(9): 379-83.

De Sousa, P. A., S. C. Juneja, et al. (1997) Normal development of preimplantation mouse embryos deficient in gap junctional coupling. J Cell Sci 110(Pt 15): 1751-8.

De Sousa, P. A., G. Valdimarsson, et al. (1993) Connexin trafficking and the control of gap junction assembly in mouse preimplantation embryos. Development 117(4): 1355-67.
Dermietzel, R. and et al. (1993) Gap junctions in the brain: where, what type, how many and why? Trends Neurosci. 16(5): 186-92. Review.

Dermietzel, R. and et al. (1998) Gap junctions in health and disease. Virchows Arch. 432(2): 177-86.

Dermietzel, R., O. Traub, et al. (1989) Differential expression of three gap junction proteins in developing and mature brain tissues. Proc Natl Acad Sci U S A 86(24): 10148-52.

Frantz, G. D. and S. K. McConnell (1996) Restriction of late cerebral cortical progenitors to an upper-layer fate. Neuron 17(1): 55-61.

Gadisseux, J. F., P. Evrard, et al. (1992) Dynamic changes in the density of radial glial fibers of the developing murine cerebral wall: a quantitative immunohistological analysis. J Comp Neurol 322(2): 246-54.

Ghosh, A. and M. E. Greenberg (1995) Distinct roles for bFGF and NT-3 in the regulation of cortical neurogenesis. Neuron 15(1): 89-103.

Kandler, K. and L. C. Katz (1995) Neuronal coupling and uncoupling in the developing nervous system. Curr Opin Neurobiol 5(1): 98-105.

Laird, D. W. (1996) The life cycle of a connexin: gap junction formation, removal, and degradation. J Bioenerg Biomembr 28(4): 311-8.

Laird, D. W., M. Castillo, et al. (1995) Gap junction turnover, intracellular trafficking, and phosphorylation of connexin43 in brefeldin A-treated rat mammary tumor cells. J Cell Biol 131(5): 1193-203.

Li, J., E. L. Hertzberg, et al. (1997) Connexin32 in oligodendrocytes and association with myelinated fibers in mouse and rat brain. J Comp Neurol 379(4): 571-91.

Lo Turco, J. J. and A. R. Kriegstein (1991) Clusters of coupled neuroblasts in embryonic neocortex. Science 252(5005): 563-6.

LoTurco, J. J. and A. Kriegstein, R. (1995). Neurotransmitter signaling before the birth of neurons. The Cortical Neuron. M. J. Gutnick and I. Mody, Oxford University Press: 197-209.

Mambetisaeva, E. T., V. Gire, et al. (1999) Multiple connexin expression in peripheral nerve, Schwann cells, and Schwannoma cells. J Neurosci Res 57(2): 166-75.

McConnell, S. K. (1995) Constructing the cerebral cortex: neurogenesis and fate determination. Neuron 15(4): 761-8.

McConnell, S. K. (1995) Strategies for the generation of neuronal diversity in the developing central nervous system. J Neurosci 15(11): 6987-98.

Menezes, J. R. and M. B. Luskin (1994) Expression of neuron-specific tubulin defines a novel population in the proliferative layers of the developing telencephalon. J Neurosci 14(9): 5399-416.

Meyer, R. A., D. W. Laird, et al. (1992) Inhibition of gap junction and adherens junction assembly by connexin and A-CAM antibodies. J Cell Biol 119(1): 179-89.

Nadarajah, B., A. M. Jones, et al. (1997) Differential expression of connexins during neocortical development and neuronal circuit formation. J Neurosci 17(9): 3096-111.

Nagy, J. I., P. A. Ochalski, et al. (1997) Evidence for the co-localization of another connexin with connexin-43 at astrocytic gap junctions in rat brain. Neuroscience 78(2): 533-48.

Nelles, E., C. Butzler, et al. (1996) Defective propagation of signals generated by sympathetic nerve stimulation in the liver of connexin32-deficient mice. Proc Natl Acad Sci U S A 93(18): 9565-70.

Pearlman, A. L., P. L. Faust, et al. (1998) New directions for neuronal migration. Curr Opin Neurobiol 8(1): 45-54.

Peinado, A., R. Yuste, et al. (1993) Extensive dye coupling between rat neocortical neurons during the period of circuit formation. Neuron 10(1): 103-14.

Polleux, F., C. Dehay, et al. (1997) The timetable of laminar neurogenesis contributes to the specification of cortical areas in mouse isocortex. J Comp Neurol 385(1): 95-116.

Rakic, P. and V. S. Caviness, Jr. (1995) Cortical development: view from neurological mutants two decades later. Neuron 14(6): 1101-4.

Ressot, C., D. Gomes, et al. (1998) Connexin32 mutations associated with X-linked Charcot-Marie-Tooth disease show two distinct behaviors: loss of function and altered gating properties. J Neurosci 18(11): 4063-75.

Risek, B., F. G. Klier, et al. (1994) Developmental regulation and structural organization of connexins in epidermal gap junctions. Dev Biol 164(1): 183-96.

Rorig, B. and B. Sutor (1996) Nitric oxide-stimulated increase in intracellular cGMP modulates gap junction coupling in rat neocortex. Neuroreport 7(2): 569-72.

Rorig, B. and B. Sutor (1996) Regulation of gap junction coupling in the developing neocortex. Mol Neurobiol 12(3): 225-49.

Rorig, B. and B. Sutor (1996) Serotonin regulates gap junction coupling in the developing rat somatosensory cortex. Eur J Neurosci 8(8): 1685-95.

Scherer, S. S., Y. T. Xu, et al. (1998) Connexin32-null mice develop demyelinating peripheral neuropathy. Glia 24(1): 8-20.

Smart, I. H. and G. M. McSherry (1982) Growth patterns in the lateral wall of the mouse telencephalon. II. Histological changes during and subsequent to the period of isocortical neuron production. J Anat 134(Pt 3): 415-42.

Stoykova, A., M. Gotz, et al. (1997) Pax6-dependent regulation of adhesive patterning, R-cadherin expression and boundary formation in developing forebrain. Development 124(19): 3765-77.

Suchyna, T. M., J. M. Nitsche, et al. (1999) Different ionic selectivities for connexins 26 and 32 produce rectifying gap junction channels. Biophys J 77(6): 2968-87.

Takahashi, T., T. Goto, et al. (1999) Sequence of neuron origin and neocortical laminar fate: relation to cell cycle of origin in the developing murine cerebral wall. J Neurosci 19(23): 10357-71.

Takahashi, T., R. S. Nowakowski, et al. (1992) BUdR as an S-phase marker for quantitative studies of cytokinetic behaviour in the murine cerebral ventricular zone. J Neurocytol 21(3): 185-97.

Takahashi, T., R. S. Nowakowski, et al. (1993) Cell cycle parameters and patterns of nuclear movement in the neocortical proliferative zone of the fetal mouse. J Neurosci 13(2): 820-33.

Takahashi, T., R. S. Nowakowski, et al. (1994) Mode of cell proliferation in the developing mouse neocortex. Proc Natl Acad Sci U S A 91(1): 375-9.

Takahashi, T., R. S. Nowakowski, et al. (1996) The leaving or Q fraction of the murine cerebral proliferative epithelium: a general model of neocortical neuronogenesis. J Neurosci 16(19): 6183-96.

Todd, P. H. and I. H. Smart (1982) Growth patterns in the lateral wall of the mouse telencephalon: III. Studies of the chronologically ordered column hypothesis of isocortical histogenesis. J Anat 134(Pt 4): 633-42.

Willecke, K., A. Temme, et al. (1999) Characterization of targeted connexin32-deficient mice: a model for the human Charcot-Marie-Tooth (X-type) inherited disease. Ann N Y Acad Sci 883: 302-9.

Yuste, R., A. Peinado, et al. (1992) Neuronal domains in developing neocortex. Science 257(5070): 665-9.

JAMES L. EUBANKS

CURRICULUM VITAE

I. ACADEMIC

EDUCATION

1994 - Present University of Washington Seattle, WA
Ph.D. expected June 2000. Neurobiology and Behavior.

1986- 1990 Colorado College Colorado Springs, CO
B.A. Biology. Minor in Comparative Literature.

HONORS/FELLOWSHIPS

1995-1999 NIH Graduate Neuroscience Training Fellow

1986-1990 Benjamin Rastall Scholar at Colorado College

DISSERTATION RESEARCH

Research Field: Developmental Neurobiology

Research Topic: The role of cell-cell communication in the development of the cerebral cortex. William J. Moody, Committee Chair

RESEARCH ROTATIONS

Laboratory of Thomas Reh: Retinoic acid receptor signaling and cell fate decisions in the developing retina.

Laboratory of William J. Moody: Acetylcholine receptor expression and spontaneous electrical activity in developing muscle.

Laboratory of Edwin Rubel: Mechanisms of cell death in the chick brainstem auditory nucleus following activity deprivation.

Laboratory of William A. Catterall: Molecular cloning of the human voltage-gated sodium channel B2 subunit; investigating its role in type 4B Charcot- Marie-Tooth disease.

TEACHING ASSISTANCESHIPS

DEPARTMENT OF ZOOLOGY • 310 KINCAID HALL • BOX 351800 • SEATTLE, WA 98195
PHONE (206) 543-7029 • FAX (206) 543-3041 • E-MAIL JEUBANKS@U.WASHINGTON.EDU

Winter 1997 Zoology 485: Animal Physiology

Winter 1998 Zoology 455: Developmental Biology

Autumn 1999 NBIO 450: Readings in Developmental Neurobiology

PUBLICATIONS

Eubanks, J., Srininvasan, J., Disteche, C., Dinulos, M., Catterall, W.A. *Structure and Chromosomal Localization of the B2 Subunit of the Human Brain Sodium Channel.* **NeuroReport** Vol.8 No. 12 2775-2779 (1997).

Bolino, A., Seri, M., Caroli, F., Eubanks, J., Srinivasan, J., Mandich, P., Schenone, A., Quattrone, A., Romeo, G. Catterall, W.A., Devoto, M. *Exclusion of the SCN2B Gene as a Candidate for CMT4B.* **European Journal of Human Genetics** Vol. 6 629-634 (1998).

PRESENTATIONS AND INVITED TALKS

November 9, 1998 Society for Neuroscience Annual Meeting, Los Angeles, CA: *Connexin Expression in the Ventricular Zone of the Embryonic Mouse Neocortex.*

September 29, 1999 International Gap Junction Conference, Thun, Switzerland: *Connexin 32 Expression in the Embryonic Mouse Neocortex and its Possible Involvement in Neuronal Migration.*

October 23, 1999 Society for Neuroscience Annual Meeting, Miami Beach, FL: *A Unique Pattern of Connexin 32 Expression Underlies Late Neuronal Migration in the Embryonic Mouse Neocortex.*

II. PROFESSIONAL

WORK EXPERIENCE (1990 TO PRESENT)

1994-Present University of Washington Seattle, WA

Research Assistant, Teaching Assistant, and Instructor

- Details listed above.

1993-1994 University of Washington Seattle, WA

Research technologist for Dr. Eliot Brenowitz, Department of Psychology

- Investigated the neuronal basis of female canary behavioral responses to male song patterns.

1992-1994 University of Washington Seattle, WA

Research technologist for Dr. John Palka, Department of Zoology

- Investigated expression of developmental genes during wound healing in Drosophila.

1991-1993 Laboratory of Pathology, Inc. Seattle, WA

Cytogenetic technologist

- Performed prenatal screening: chromosome analysis of fetal cells derived from amniocentesis (samples of amniotic fluid).

1990-1991 The Beeliner Diner Seattle, WA

Lipids Engineer (Fry Cook)

- Specialized in the thermodynamically induced hydrolysis of culinary substrates.

VOLUNTEER EXPERIENCE

- Outreach worker for homeless youth in Seattle through Street Links, a program of Seattle Children's Home.
- Science Instructor for the Upward Bound program.
- Coordinator and participant for Seattle Works Day, a yearly city-wide volunteer-a-thon.

PROFESSIONAL MEMBERSHIPS

- Society for Neuroscience
- American Physiological Society